STEWART, JONATHAN A., M.S. Inhibition of Cytochrome P450 Subfamilies 2E1, 2A6, & 2B4 Using the Amazon Acai Berry, *Euterpe oleracea*. (2010)
Directed by Dr. Gregory M. Raner. 72 pp.

The ability for cytochrome P450s to metabolize drugs and other compounds foreign to the body has led scientists to monitor the metabolites formed from the metabolic cycle of xenobiotics as they can prove potentially fatal if produced in large quantities. These by-products of P450 metabolism have been found to be the cause of the formation of reactive oxygen species (ROS's) and their role in the up-regulation of cancer cells and denaturing of nucleic acids. The use of essential oils to slow down or inhibit P450s has shown some light on dietary restrictions while taking a drug regimen. Aldehydes are a main chemical constituent in essential oils and have been known to inhibit P450s. Inhibiting the catalytic cycle that P450s undertake prevents or slows the formation of toxic by-products. The amazon berry *Euterpe oleracea*, commonly known as the acai berry, has shown to have positive health benefits in people who make it part of their diet. Knowing that acai has potential antioxidant properties, the extraction of acai oil from freeze dried *Euterpe oleracea* was used to probe P450 inhibiton in the 2E1, 2A6, and 2B4 isoforms. The results from this study suggests that acai inhibits these P450s but in a mixed-inhibitor mechanism where the most probable route of inhibition occurs directly at the active site or some allosteric site that directly suppresses enzyme activity. Using GC-MS/MS, the acai oil contains >55% aldehyde composition, suggesting that these compounds are possible inhibitors for P450s probed in this study.

INHIBITION OF CYTOCHROME P450 SUBFAMILIES 2E1, 2A6, & 2B4 USING THE AMAZON ACAI BERRY *EUTERPE OLERACEA*

By

Jonathan A. Stewart

A Thesis Submitted to
The Faculty of The Graduate School at
The University of North Carolina at Greensboro
In Partial Fulfillment
Of the Requirements for the Degree
Master of Science

Greensboro
2010

Approved by

_____
Committee Chair

APPROVAL PAGE

This thesis has been approved by the following committee of the Faculty of The Graduate School at The University of North Carolina at Greensboro.

Committee Chair _____

Committee Members _____

_____

_____

Date of Acceptance by Committee

_____

Date of Final Oral Examination

ACKNOWLEDGEMENTS

The author extends his thanks and gratitude to the following individuals for serving as committee members and providing assistance and guidance: Dr. Gregory Raner (Chairman), Dr. Nadja Cech, and Dr. Nicholas Oberlies.

TABLE OF CONTENTS

Page

LIST OF FIGURES

Page

CHAPTER I

INTRODUCTION

1.1.0 Cytochrome P450s & Metabolism

The ability of all vertebrates to prevent the unwanted accumulation of foreign chemicals (xenobiotics) and free radicals is attributed to the presence of naturally occurring detoxifying enzymes known as the cytochrome P450s – so named because their UV-Vis spectra are characterized by a strong absorption band detected at or around 450 nanometers in their reduced-CO bound state (1). Located in the smooth endoplasmic reticulum as well as the inner mitochondrial membrane in cells of smooth muscle tissue and, most notably, hepatocytes, cytochrome P450s (abbreviated CYPs) form a class of enzymes known as heme monooxygenases where molecular oxygen is used to deactive exogenous substances, forming water and an alcohol as by-products of Phase I xenobiotic metabolism (2).

The effectiveness of CYPs in degrading pharmaceutical agents has drawn scientists to study this process with regard to the formation of chemical by-products that have the potential to cause adverse effects in the host. Notable examples of drugs that may be activated to form more toxic products include acetaminophen, valproic acid, and

dextromethorphan (3, 30). Drugs in particular may be converted by these enzymes into chemical by-products that may or may be dangerous to the host (3). These metabolites can include epoxides and free radical species having the potential to form DNA adducts (4). Certain xenobiotics or metabolites may cause a variety of effects that include the up-regulation of gene expression, which can have significant physiological consequences as well (5).

Cytochrome P450s are the major enzymes in the body that act to inactivate drugs during metabolism and are likely responsible for the production of toxic by-products of foreign compounds where xenobiotics are present (6). Thus, it may be beneficial to reduce the activities of this particular family of enzymes that are responsible for such activation. An important feature of P450s is that they require a reductase which aids in reduction of the iron atom at the core of the heme cofactor within the porphyrin ring (7). NADPH-cytochrome P450 reductase (CPR) is the simplest membrane-bound reductase that aids in P450 reduction by accepting a pair of electrons from NADPH via a hydride ion. The electrons are then shuttled through the reductase in a process mediated by the effects of the cofactors FAD and FMN. Both cofactors transfer electrons one at a time to the P450 isozyme where, when combined with molecular oxygen, chemical oxidations, most notably hydroxylations, are observed on the substrate when it binds to the active site (8). Before introducing any means to inactivate or slow the production of xenobiotic metabolism it is necessary to discuss the two types of metabolism, phase I and phase II metabolism.

During phase I metabolism, a drug or other exogenous compound is chemically altered, usually via oxidation. Cytochrome P450 enzymes are the major class of Phase I enzymes in the body. P450 enzymes contain a heme protoporphyrin IX ring with a Fe^{+3} ion that is bound to four adjacent nitrogen atoms that make up the porphyrin core (9). This gives rise to the brilliant red-to-orange color associated with P450 enzymes (8, 9).

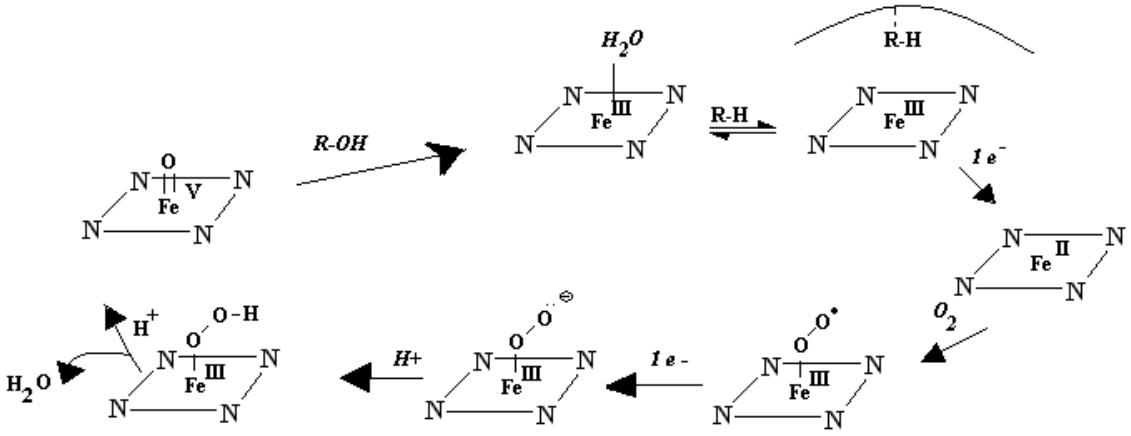

Figure 1. P450 catalytic cycle depicting the initiation steps resulting in hydroxylation of a substrate. Adapted from reference 1

Present in the biological matrix is the cofactor NADPH which is associated with the CPR and serves as the electron donor. Once molecular oxygen is present, the CPR initiates binding of the O_2, to the active site where the formation of an oxo-ferryl (Fe^{+5}=O) intermediate is initiated (1). Figure 1 shows the catalytic cycle where the heme group is tethered to the apoprotein within the P450 via a thiolate ligand (not shown) which is provided by a neighboring cysteine residue in the active site (6). The catalytic

cycle for P450 enzymes involves the substrate coming into close proximity of the active site, displacing a bound water molecule. This converts the ferric-heme from a low spin to a high spin state (10). The change in the electronic state of the iron is responsible for the spectroscopic shift in the wavelength for the Soret peak of the heme from 418nm to 390nm (11). Once in the high-spin state an electron transfer from NADPH results in the ferrous-heme complex (10, 11).

The initiation step involved in the catalytic cycle for P450s involves a two electron reduction of molecular oxygen to form water and an oxygen reactive species (1). Molecular oxygen covalently binds to the distal heme position of the ferrous protein where a second electron is transferred from the reductase constituent, forming a peroxo-iron complex. The peroxo intermediate undergoes a heterolytic bond cleavage where the ferric-heme iron is oxidized to the Fe^{+5}state (1, 6). At this point in P450 catalysis a reaction occurs where the iron-oxo species abstracts a hydrogen atom from the substrate to form a radical (6). The resulting Fe^{+4}-OH then transfers the hydroxyl substrate radical, resulting in hydroxylation where the iron is reduced back to the Fe^{+3}state (1).

1.2.0 Reactions of P450s

The reactions in which P450s participate can be classified according to the functional groups associated with the substrate. Since most drugs have characteristic functional groups, chemists have proposed mechanisms and computational models to help visualize these simple-to-complex organic reactions. There are more than twenty chemical oxidations reported for P450 catalyzed reactions (1).

Reaction models and mechanisms associated with P450 metabolism listed in the figures in the following pages depict the substrate (the alcohol, aldehyde, etc) interacting with the heme moiety associated with the active site. The oxidation steps are a result of the reductase interacting with the P450. Protonation or deprotonation of the substrate occurs with the aid of the active site amino acid residues.

The majority of substrates for P450s contain functional groups that may or may not be selective for a particular isozyme. Many different substrates have different effects for a particular isoform, all which proceed in a step-wise mechanism. For the purposes of this research, I will discuss the following classes of reactions that P450s metabolize: Aldehyde oxidations; Aromatic (hydrocarbon) hydroxylations reactions; dehydrogenation reactions.

1.2.1 Aldehyde Oxidations in P450s

It has been shown that P450s catalyze many oxidation reactions and aldehyde oxidation is one prime example. The compound cyclohexanecarboxaldehyde is oxidized by the chytochrome P450 isoform 2B4 (formally written as CYP_{2B4}) where hydroxylation occurs at the carbonyl to produce the corresponding carboxylic acid (12). The reaction mechanism is illustrated in Figure 2. Interestingly, in this reaction a second reaction pathway has been proposed in which the peroxo-iron species, prior to undergoing heterolytic O-O bond cleavage, appears to represent the oxidizing species rather than the Fe+5=O ferryl species. A nucleophilic attack on the carbonyl,in addition

to the Fe-O-O intermediate, may be involved, initiating the formation of a peroxyhemiacetal (13) . The ß oxygen from the iron (due to proximity) abstracts the neighboring hydrogen from the cyclohexyl group, forming a double bond between C2 and C3, liberating formic acid and leaving Fe^{+3}-OH. This is a concerted reaction that occurs with certain aldehyde substrates and serves as a basis for understanding the mechanisms involved in steroid metabolism (14).

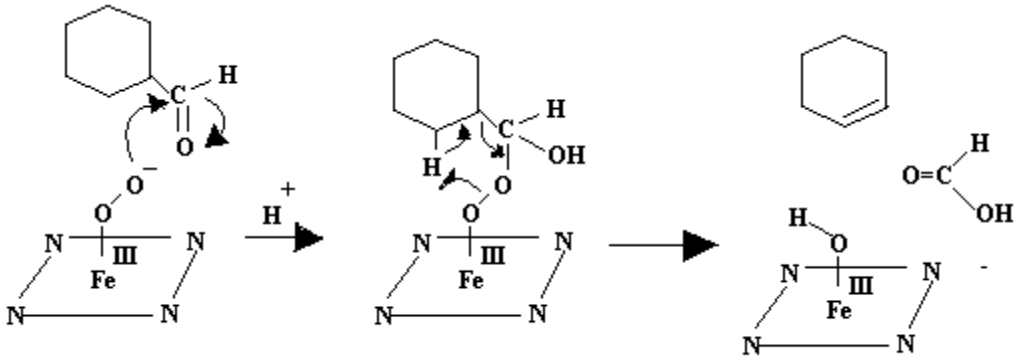

Figure 2. Mechanism for aldehyde oxidation via P450 catalysis. Adapted from Reference 15

1.2.2 Aromatic Hydrocarbon Hydroxylations

A majority of substrates for P450s are aromatic and are relevant to the research described in this document. Para-nitrophenol, a substrate metabolized by CYP_{2E1}, will be used as a model for describing aromatic reactions. In this reaction mechanism, hydrogen is abstracted from the C2 position of the aromatic ring resulting in the formation of a transient radical that undergoes a "rebound" reaction with the resulting hydroxylated

iron-(IV) species (see Figure 3a). To further describle hydroxylations by P450s, an alternate mechanism for the formation of phenol from benzene has been proposed by Jerina et al at the National Institute of Health, where the proposed "NIH shift" of deuterium is shown in Figure 3b. During P450 catalysis the formation of a Fe+4 radical cation initiates formation of a bond yielding a radical at the C2 position. The radical transfer then liberates the Fe+4 to the Fe+3 state to form a carbocation. One of the hydrogens associated with the carbon at the carbocation initiates the formation of a double bond, regenerating aromaticity and the doubly bonded oxygen will pick up a proton from an acidic species in the active site (2).

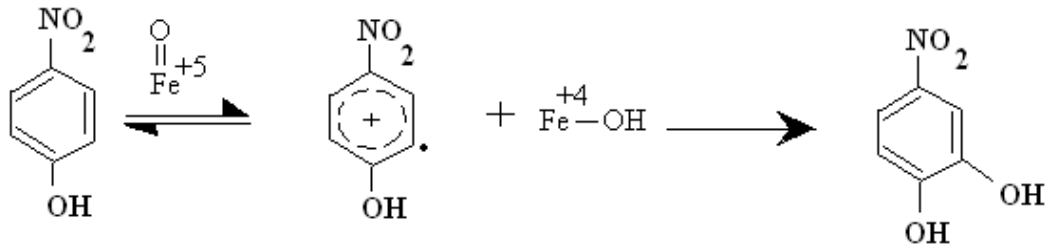

Figure 3a. Proposed mechanism for aromatic hydroxylation by P450s. Adapted from reference 16

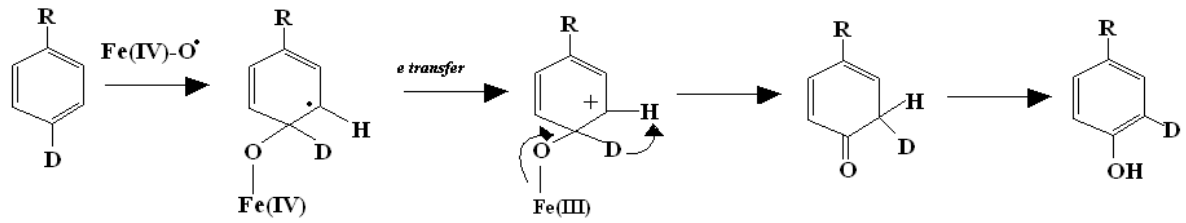

Figure 3b. Mechanism illustrating the NIH shift resulting in hydroxylation of benzene. Adapted from reference 1

1.2.3 Dehydrogenation Reactions

Another type of reaction that P450s undergo is dehydrogenation where molecular oxygen is converted into water to generate an alkene. As the name *dehydrogenation* implies, the reaction involves hydrogen abstraction to form a double bond (17). In the example of 3-methylindole (Figure 4) a hydrogen is removed from the methyl group of C3 on the indole molecule where a radical is formed. The iron from the P450 yields a single electron transfer, generating a methyl-carbocation on C3. At the same time this rate-determining step promotes Fe+4 to Fe+3 where the hydroxyl group remains bound to the metal center. Alternatively, following the initial H-abstraction, a "rebound" step may occur as with p-nitrophenol (see Figure 3) resulting in the hydroxylated product. An electron transfer will occur where, in a rebound reaction, the hydrogen on the hydroxyl group of the Fe+4 is transferred back to the methyl-carbocation, forming a double bond between C3 and C4 to yield 3-methyleneindolenine (18).

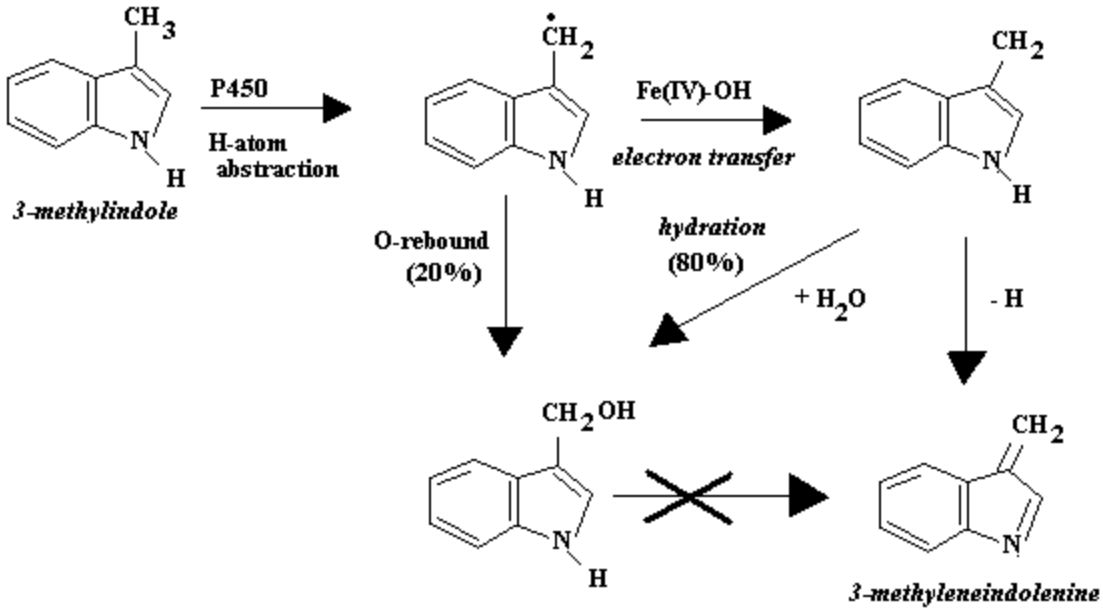

Figure 4. Formation of 3-methyleneindolenine via P450 dehydrogenation. Adapted from reference 17.

1.3.0 Inhibiton of Cytochrome P450s

Drug metabolism has been studied in great detail over the past few decades and knowledge of altered drug breakdown has been greatly studied as well. Concern for drug-drug or drug-food interaction has brought about issues regarding the P450s and P450 inhibition. A study conducted in 1989 found that patients on drug regimen who consumed grapefruit and grapefruit juice experienced increased bioavailability from drug therapy due to the high polyphenolic composition of grapefruit (19). Further studies helped identify compounds such as bergamottin and dihydroxy-bergamottin, which were responsible fogggr this enhanced bioavailability due to P450 inhibition (20). Mechanistic

studies showed that the alterations in drug metabolism were the direct result of irreversible chemical destruction of the heme associated with CYP3A4 (22). Clearly an understanding of potential interactions between natural products and drug metabolizing enzymes is very important for avoiding these types of interactions. This is especially true for interactions between natural products and pharmaceuticals, as the use of both is extensive in the U.S. population where more and more individuals are turning to natural products to treat minor illnesses or in preventing major ones (33).

There are many ways in which small molecules can influence the catalytic activity of an enzyme. The type of inhibition observed with certain chemical functional groups is of high importance in these CYP studies as they aid computational and theoretical chemists in developing models for the type of activity that is present upon taking a drug and consuming natural products in every-day diet.

The Michaelis-Menton model in Figure 5 serves as a representation of enzyme inhibition, though, using a Michaelis-Menton plot the overall behavior can be observed from data generated from a kinetic reaction. From Michaelis-Menton kinetics the maximum rate of free enzyme, V_{Max}, is plotted against the reaction of enzyme incubated in the presence of inhibitor, known as V_{Max}^{app}. The magnitude of inhibition is the result in a decrease in V_{Max} and the value of K_M – defined as the concentration of substrate at half the maximum velocity (24). Both of these values provide information regarding the type of inhibition for the P450 analyses.

There are three main types of inhibition: Reversible; Quasi-reversible; Irreversible (22, 23). The equation in Figure 5 represents a Michaelis-Menton model for the three types of inhibition used to predict the behavior of the P450s studied in this research. Reversible inhibition occurs when a compound or molecule binds to the enzyme active, site similar to a substrate binding to the same active site, where binding interferes with normal metabolic activity.

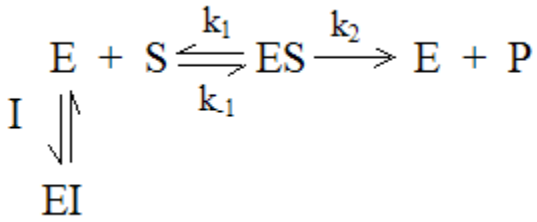

Figure 5: Michaelis-Menton model introducing an inhibitor for enzyme reaction process. Adapted from reference 24

The formation of the ES complex is prevented in this case by the equilibrium between the enzyme and inhibitor (E + I) where the free enzyme is pulled into an inhibitor-bound (EI) complex, resulting in no covalent binding. Thus, by simply removing the inhibitor from the reaction, product formation can resume (24).

The primary characteristics observed for simple competitive inhibition are that the maximum velocity of the reaction is unchanged; however, the K_M in the presence of an inhibitor is increased significantly. This is most easily observed by taking the inverse of

the raw data to generate a double reciprocal (Lineweaver-Burke) plot where both curves intersect on the *x* and *y-axes*.

The relation depicted in the equation below shows the relationship between the dissociation constant K_D, the inhibition constant K_I, and the ration of the [E][I] versus the concentration of [EI]. Here K_I is a measure of the potency of the inhibitor.

$$K_D = K_I = \frac{[E][I]}{[EI]}$$

Equation 1: Relationship between the binding constant K_D to the ratio of the concentration of enzyme and inhibitor. Adapted from reference 24

Quasi-irreversible inhibitors include molecules that contain a heteroatom that binds to the iron atom associated with the heme prosthetic group of the P450. This type of inhibition depends upon the oxidation state of the iron in that the more oxidized the iron the stronger the inhibition and vice versa (25).

Irreversible inhibition is another type of inhibition that involves the formation of a stable covalent bond between the enzyme and the inhibitor. The complex is either less active than the unmodified enzyme or completely inactive. A typical mechanism by which irreversible inhibition of P450s occurs is via alkylation or acylation of the side chain of active site residues, or via chemical modification of the heme cofactor itself (26). There are many examples of irreversible inhibitors. A subtype of irreversible inhibition

is referred to as “mechanism based” inhibition, or “suicide” inhibition. In this type of inhibition, the inhibitor must first undergo an ezyme-catalyzed chemical transformation, which activates the inhibitor, making it more reactive (24). Because cytochrome P450s employ a very strong oxidant in the cause of fulfilling their metabolic role, they are particularly promiscuous in terms of substrate recognition, having a high tendency to promote unwanted side reactions that generate species capable of reacting in this way (1, 23, 24,).

Cytochrome P450s have been studied since the 1940s by pharmacologists and biochemists as the market for drug manufacturing increased tremendously during the early 1940 and late 1980s (27). Toxicology studies and years of research has recognized CYPs to catalyze a wide range of oxidative and reductive biotransformations via the reactions previously mentioned as well as other reaction mechanisms (28). Understanding the mechanisms and modes of inhibiting P450s may shed some light in the development of new pharmacological agents.

1.4.0 Objective Statement

As mentioned earlier, inhibition studies are a significant component of drug interaction studies. The use of essential oils and other natural products has been increasing in recent years, yet studies aimed at evaluating potential interactions between these products and P450 enzymes is lacking; thus, this was a primary general objective for this study. The P450s that were probed in this research were $CYP_{2E}1$, CYP_{2A6}, and CYP_{2B4}, all responsible for the metabolism of a vast number of compounds found in

tobacco (CYP_{2E1}) and medications (CYP_{2B4} and CYP_{2A6}). The 2E1 isozyme plays a key role in the conversion of nitrosamines into carcinogenic species (29, 30). Nitrosamines, which are found in tobacco products, are also metabolized by CYP_{2A6} into cytotoxic by-products. A study conducted by Weymern and Hollenberg used a variety of phenyl-isothiocyanates (PITCs)-compounds found naturally in cruciferous vegetables- to probe inhibition of 2E1 and 2A6. Their results showed that using 10μM concentration of t-BITC (tert-butyl isothiocyanate) directly inhibited CYP_{2A6}, suggesting that substrate structure and molecular activity with the active site is the key to understanding P450 inhibition mechanism (30). They also concluded, by an extension of these results, that the beneficial effects of PITCs were in part due to reduction in 2E1 and 2A6 activities (30).

Numerous berry oils and juices contain polyphenols found to be good inhibitors of CYPs. Inhibitors of certain CYP isoforms have shown to prevent formation of damaging free radicals and toxic by-products in the body (2). The polyphenolic composition of natural plants and plant extracts contain reknown compounds such as ellagic acid, which has recently proven to induce apoptosis in proliferating pancreatic cancer cells (31). Further research has shown that antioxidant flavonoids and carotenoids, when used in conjunction with vitamin C, enhance the free radical uptake by a mechanism not yet understood and may prove effective at treating certain cancers (32). Spices such as cinnamon contain beneficial aldehydes such as cinnamaldehyde and have been used for years to treat bacterial infections in tropical regions of the world (33).

A specific objective of the current study was to evaluate the effects of acai berry extracts and essential oil on CYP_{2E1}, CYP_{2A6}, and CYP_{2B4} activity. A major hypothesis on which this research is based is that the acai berry contains constituents that strongly inhibit the action of CYP_{2E1} and CYP_{2A6}, and that this inhibition contributes to the overall anti-oxidant properties observed for the berries. For many centuries, berries have proven to alleviate certain ailments and prolonged life for many cultures (34). One such berry in the South American-Amazon region has been used as a panacea for many years. The acai berry, *Euterepe oleracea*, is a type of palm fruit that is known for its high antioxidant capacity, possibly related to its high concentration of polyphenolics and anthocyannidin (ACN) content (34, 35, 36). According to a study done by Pacheco-Palercia et al at Texas A&M University, research findings indicated that acai berry contained phytochemicals known to retard or halt carcinogenesis, among them protocatechuic acid, p-hydroxybenzoic acid, (+)-catechin, vanillic acid, syringic acid, and ferulic acid (34, 37). Contrary to these findings, a team of researchers from AIMBR Life Sciences identified five major anthocyanidins using freeze-dried acai berry. Among the compounds found were cyanidin- 3-sambubioside, cyanidin- 3-rutinoside, peonidin- 3-glucoside, peonidin- 3-rutinoside, and cyanidin- 3-glucoside. This study indicated that the total ACN content in acai berry was low, suggesting that their biochemical response in the previously identified *in vitro* assay would not be significant (36).

The composition of acai berry juice, once homogenized, consists of a non-polar layer, which contains the essential omega-fatty acids oleic and linoleic acid, an aqueous

layer containing water-soluble phytochemicals, and the pulp whose constituents are mostly proto-anthocyanidins (36). Based on current research there is an overall abundance of essential nutrients that can target CYPs by some form of inhibition.

There are two components to my research involving both a qualitative and a quantitative approach. Identifying specific phytochemicals in both the acai oil and the aqueous fraction is the focus for the qualitative approach as well as observing the type of inhibition model each P450 isoform fits. In addition to the inhibition studies the IC50, more specifically the potency, of the acai oil for each P450 will be obtained by an initial screening, representing the quantitative aspect for this research project.

Gas chromatography has served as a powerful tool for identifying unknowns (12). As previously mentioned, identifying the natural compounds in both the oil and the aqueous extracts will be vital for attempting to identify possible inhibitors, if any, for the P450s studied in this project. By comparing both GC components and the Michaelis-Menton results the selection for naturally occurring compounds in the berry will be used to help identify potential inhibitors of P450s.

CHAPTER II

EXPERIMENTAL

2.1.0 Preparation of Reagents

2.1.1 Preparation of Phosphate Buffer. Potassium phosphate buffer was a combination of both monobasic phosphate buffer purchased from RICCA Chemical & Co. and dibasic phosphate buffer which was purchased from Fisher Scientific, Inc. and adjusted to pH 7.45. A 1 M stock solution of potassium phosphate (pH 7.4) was used in the preparation of both screening reactions and Michaelis-Menton kinetic assays described in the following sections.

2.1.2 Preparation of P450 Enzymes. Rabbit liver microsomes were prepared as discussed by F. P. Guengerich, et al (10). A 4:1 ratio of rabbit liver (weighing 70g) and 0.05 M potassium phosphate buffer (pH 7.4) was prepared by blending in a blender and subsequently centrifuged for 10 min at 5000rpm. The supernatant was decanted into an additional mixing vessel and centrifuged at 20,000rpm for 1 hour. The suspended pellet (approximately 1mL) was transferred into a homogenizer and reconstituted to 30 mL with buffer. The mixture was blended until homogeneous and the microsomes were stored at -70°C.

2.1.3 Preparation of NADPH. High purity NADPH, purchased from Sigma-Aldrich, was prepared by weighing out 16.7mg and dissolved in 1mL of deionized water to make a 20mM stock solution.

2.1.4 Preparation of p-nitrophenol. Roughly 0.139g of p-nitrophenol (purchased from Sigma-Aldrich) was dissolved in 10mL of high-purity grade methanol (Fisher Scientific) where 10µL was dissolved in 10mL of deionized water to make a 1mM solution.

2.1.5 Preparation of 1,2-Benzopyrone Stock Solution. Coumarin (1, 2-benzopyrone) was purchased from Sigma. For the reaction assays for CYP_{2A6}, 0.0014g of 1,2-benzopyrone was weighed and dissolved in 1mL of methanol to give a 0.01M stock solution. Finally, 100µL of the 0.01M stock was reconstituted to a final volume of 1000µL of deionized water to give a final concentration of 1mM which was used in the reaction.

2.1.6 Preparation of N,N dimethylaniline Solution. High purity (99% grade) N, N-dimethylaniline was purchased from Aldrich Chemical Company and was the substrate used for CYP_{2B4} assay. A 10mM solution was prepared by dissolving 63µL of N, N-dimethylaniline to 49.937mL of water.

2.1.7 Preparation of Nash Reagent. The Nash reagent was used in the CYP_{2B4} assay to aid in the quantification of formaldehyde where the substrate, N, N-dimethylaniline, is metabolized into N-methylhydroaniline and formaldehyde. The reagent was prepared by

weighing out 15g of sodium acetate and adding 200μL of 2,4-pentandione. The mixture was vortexed for 2-3minutes and was stored at room temperature.

2.1.8 Preparation of Benzyl Alcohol Solution. A 12μL aliquot of 99% benzyl alcohol (purchased from Acros Organics, Inc) was dissolved in 10mL of deionized water to obtain a 12 mM stock solution. A 1mL aliquot of the 12mM stock was dissolved in 10mL of deionized water to generate a 1.2mM solution which was used for the CYP_{2B4} assay.

2.1.9 Preparation and Extraction of Acai Oil. Freeze-dried acai, Euterpe oleracea, was purchased from Optimally Organic. Roughly 5g of freeze-dried acai was weighed out and dissolved in 50mL of deionized water. The mixture was centrifuged at 35,000 rpm at 10°C for 15 minutes. The aqueous supernant was decanted into a 120mL separatory funnel in which 50mL of chloroform was added. The solution was shaken for 3 minutes and allowed to sit in order to separate both aqueous and organic layers. The organic layer, whose density was greater than the aqueous, was eluted from the separatory funnel and collected into a receiving flask. This liquid-liquid extraction process was repeated two more times with 50mL aliqouts of chloroform until roughly 150mL of extract was collected.

The extract was filtered into a round- bottom flask using anhydrous sodium sulfate to collect any aqueous residue. The extract was evaporated using a rotor evaporator (Buchi Scientific Instruments) where the acai oil was formed as the

chloroform evaporated. The oil was transferred into a micro-centrifuge tube and stored at room temperature.

2.2.0 Characterization of Aqueous Fraction of Acai. Acai juice consisting of 100% juice from certified organic acai, pomegranate, apple, grape, cherry, and blueberry was purchased from a local food store, where 50 mL of the juice was transferred into a centrifuge tube and centrifuged at 3500 rpm for 30 minutes. A 3mL aliquot of the aqueous supernant was transferred into a Waters Oasis MCX cartridge and pulled through under vacuum. The retained compounds from the cartridge were eluted using a 90:10 methanol/water rinse solution, where 1mL of the eluent was dissolved in 20mL of methanol and ran on GC-MS for analysis. The GC chromatogram for the acai juice extracts are shown in Figure 6.

2.2.1 Preparation of Acai Oil Solution. Using an automatic pipette, 10µL of oil was dissolved in 190 µL of methanol with an additional 800 µL of water. This stock solution was then reconstituted with deionized water to 100 mL that gave a concentration of 80µg/mL. *Lakewood® Organic Acai Amazon Berry Juice* was purchased at a local health food store where the aqueous supernatant was used as the inhibitor for CYP_{2E1} only.

2.3.0 Quantitative Measurements. The metabolites from the CYP2E1 and 2A6 catalyzed reactions were analyzed using a Shimadzu High Performance Liquid Chromatograph equipped with a SIL-20A/20AC autosampler, UV-Vis detector and a

built-in solvent delivery system. All data was quantified by integrating the peak areas from each chromatograph and comparing them to a known standard. An Agilent Zorbax SB-C8 4.6 x 150mm column with 5µm pore size was used for both CYP_{2E1} and CYP_{2A6} assays. Calibration curves were generated for all standards in order to measure instrument sensitivity; the measure of linearity for 7-hydroxycoumarin and p-nitrocatechol gave R^2 values of 0.9913 and 0.9999 respectively.

2.3.1 Method Parameters. The following sections discuss the reaction conditions and settings for the HPLC-UV-Vis system.

2.3.2 p-Nitrocatechol Assay. For the CYP_{2E1} assay the reaction was carried out at 37°C and allowed to incubate for 30 minutes following the addition of 1mM NADPH in the presence of 50 mM phosphate buffer, 25 µL rabbit liver microsomes, and p-nitrocatechol (20 – 160 µM). In addition to a set of control samples were samples that had the same reagents mentioned plus 0.8mg/mL acai oil solution. The reaction was quenched with 200µL of 6% perchloric acid and allowed to cool on ice for 10 minutes. The HPLC method used to measure the amount of p-nitrocatechol produced is as follows: Method run time was set to 8 minutes, with an isocratic gradient and a flow rate set at 0.6mL/min; Solvent A (aqueous) was set at 35% water with 0.5% acetic acid; Solvent B (organic) was set at 65% acetonitrile with 0.5% acetic acid; The UV detector was set at 340nm. The retention time for p-nitrocatechol using these parameters was 0.450 min using 8 minute runtime using a 150 x 3.2 mm, 5 µm pore-size C18 column purchased from Varian.

2.3.3 Coumarin Assay. Samples were incubated at 37°C for 30 minutes in the presence of 1mM NADPH, 50 µL of 1 M phosphate buffer, 25 µL rabbit liver microsomes, 80 µg/mL acai oil solution, and 0.02mM – 0.2mM coumarin for a 500µL reaction volume. Samples were quenched with 200 µL 6% perchloric acid and allowed to cool on ice for 10 minutes. The HPLC conditions were as follows: Flow rate set to 0.6mL/min; UV detector set at 320nm; run time set at 10 minutes. The mobile phase was also isocratic with solvent A (water) at 45% water with 0.5% acetic acid and solvent B (methanol) at 55% with 0.5% acetic acid. The retention time for 7-hydroxycoumarin was 1.417min and 2.783min for coumarin using a runtime of 8 minutes using a 4.6 x 250 mm, C8 column purchased from Agilent.

2.3.4 CYP_{2B4} Assay. Samples were incubated at 37°C for 30 minutes in the presence of 50 µL phosphate buffer, 25 µL rabbit liver microsomes, 16 µg/mL acai oil solution, and 50 - 200 µL aliquots of 5mM N,N-dimethylaniline in a 500µL reaction tube. Samples were then quenched with 250 µL 6% trichloroacetic acid and cooled on ice for an additional 30 minutes. Samples were then centrifuged at 3500 rpm for 10 minutes where the supernatant was added to 400 µL Nash reagent and allowed to incubate at 37°C for 30 minutes. The concentrations of formaldehyde were measured using a Cary 100 UV/Vis spectrophotometer. Samples were scanned from 500 nm to 300 nm where the target wavelength was 412 nm. The concentration of each sample was calculated using Beer's law. The molar absorptivity used to calculate the analyte concentrations was 0.110 $\mu M^{-1} cm^{-1}$.

2.3.5 Benzyl Alcohol Assay Using CYP_{2B4}. An alternative to the Nash assay is the metabolism of benzyl alcohol into benzaldehyde. This analysis was based on an HPLC assay in which the microsomes were incubated in the presence of 0.15 – 0.30mM benzyl alcohol. The reaction was incubated in the presence of pH 7.2 0.1M phosphate buffer in a 500µL tube for 30 minutes and quenched with 200µL of perchloric acid. The reaction was then centrifuged at 35000 rpm, and the supernatant vialed for HPLC analysis. The retention time for benzaldehyde was 2.067min for a 6 minute runtime using a 150 x 4.6 mm, C8 column purchased from Phenomenx.

2.4.0 Characterization of Unknown Compounds in Acai Oil.

The qualitative aspect of this research involved separation of unknown analytes in the acai oil. This was accomplished using a Shimadzu GCMS-QP2010S Gas Chromatograph equipped with a quadrupole mass-spectral detector. A RTX-5 amine Crossbond (5% diphenyl/95% dimethyl polysiloxane coating) column that was purchased from Restek was used in the separation of individual compounds. The operating conditions of the GC/MS are as follows: Splittless injection; 100kPa helium gas pressure; flow rate set to 50mL/min; ion source and interface temperatures were set to 250°C; inlet temperature was set at 35°C and was ramped to 325°C and held for 5 minutes concluding the 30 minute run time; MS scan from 50m/z to 500m/z. A 10µL aliquot of the acai oil was dissolved in 1mL of chloroform where a 1µL injection was used for GC analysis.

CHAPTER III

RESULTS AND DISCUSSION

3.1.0 Qualitative Data from GC/MS

As previously stated one of the goals of this study was to characterize the essential oil components of acai berry. Previous research on other essential oils suggests the presence of a very diverse array of aromatic and unsaturated compounds, especially terpenes, polyphenols and fatty acids. Many of these compounds have been proposed to elicit positive health effects in humans. For example, syringic acid and vanillic acid are compounds that have been separated from olive oil whose organoleptic properties are believed to play an important role in disease prevention (34).

The freeze-dried acai berry, after undergoing liquid-liquid extraction, separates into an aqueous phase, organic phase and a pulp phase in a separatory funnel. The aqueous phase consists of the hydrophilic phenol groups, sugars and anthocyanidins (34). The organic phase is a suspension of organic solvent containing nonpolar compounds and suspended oil particulate that settles at the bottom of the separatory funnel. The fraction containing the pulp is partitioned between the organic and aqueous phases. Roughly 1.2

mL of oil was obtained after extraction. It mainly consists of fiber, sugar components, and hydrophobic compounds (35).

3.1.1 Characterization of Aqueous Phase Using Gas Chromatography

An attempt was made to identify compounds in both the aqueous phase and the fraction containing the oil from the acai solution. The aqueous phase components were separated using a Waters HLB solid phase extraction cartridge where the retained analytes were eluted with 99.5% methanol 0.5% acetic acid solution. The eluant was transferred into 1.5mL microcentrifuge tubes and evaporated under reduced pressure using a Savant SC110 Speed Vac until dry. To the dried material, 1mL of chloroform was added and the contents were shaken until fully dissolved. The sample was then analyzed by GC/MS in an attempt to identify specific chemical constituents. Figure 6 displays the total ion count for the aqueous injection as described.

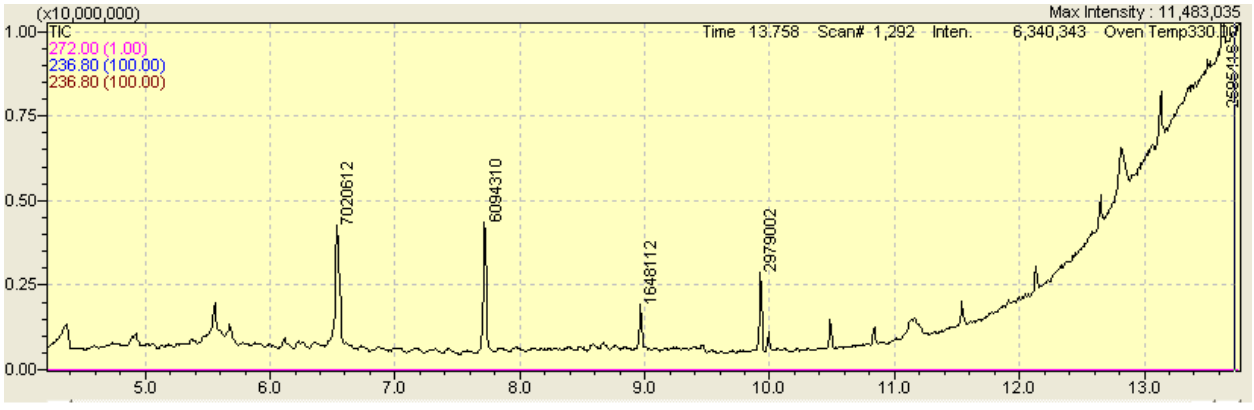

Figure 6. Total ion chromatograph for solid phase extraction of aqueous fraction of acai juice

The compounds of interest were identified using the spectral library NIST program. The values above each peak are auto-integrated areas. The compound separated at 6.58 minutes was identified as 3,5,7-trimethoxy-2-(4-methoxyphenyl)-4H-1-benzopyran-4-one. The compound at 7.75 minutes was identified as 2-benzo(1,3)dioxol-5yl-8-methoxy-3-nitro-2H-chromene. These compounds are known derivatives for the precursors for tannins – a group of phytochemicals believed to be responsible for overall antioxidant activities. Tannins are predominantly found in fleshy fruits, teas and red wine (38). The compound separated at 8.91 minutes was identified as 3,4-dihydroxymandelic acid. The compound at 9.86 minutes was identified as 6-chloro-4-phenyl-2-propylquinoline. The compound at 10.49 minutes was identified as scutellarein tetramethyl ether. The following peaks were the result of column bleed from increasing temperatures and possible water particulate on the GC column.

3.1.2 Characterization of Acai Oil Using Gas Chromatography

The organic phase was of particular interest as the acai oil was miscible in chloroform. The generation of the acai oil is discussed in section 2.1.8. Figure 7 is a chromatogram showing the total ion count for the acai oil extracted from freeze-dried acai berry. The analytes and their retention times are listed in the order that they elute from the GC column.

The peaks observed from zero minutes to 3 minutes were identified as isotopes for the solvent chloroform and were subtracted from the background. Interestingly, the oil contained a large variety of different non-polar organic compounds and only a couple

polar compounds were identified. All compounds were identified according to their fragmentation patterns and were match with the NIST fragmentation spectrum that best corresponded to the target spectrum. Aldehydes were abundantly present from the beginning of the run up to approximately 15 minutes where other nonpolar compounds began to elute until the run was complete. Sections of the GC scan displaying individual compounds are shown in the following figures.

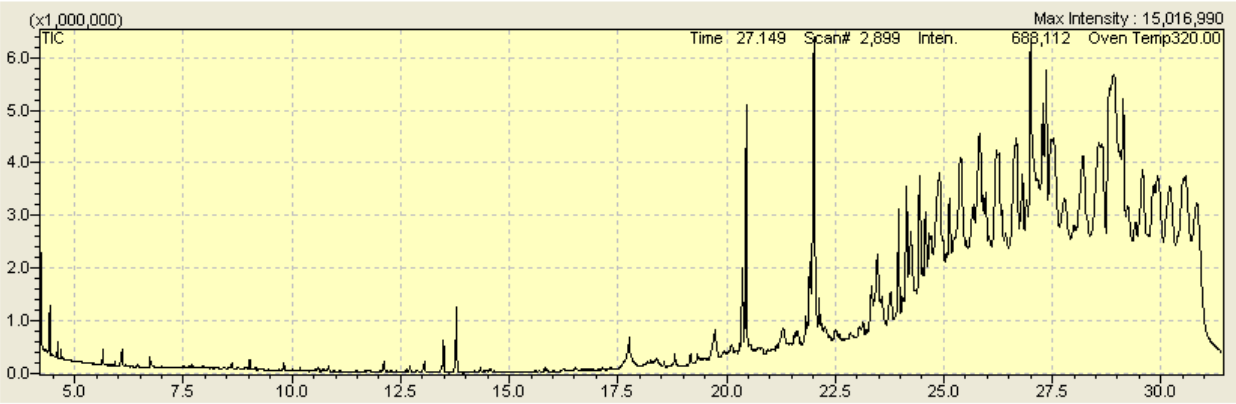

Figure 7. Total Ion Chromatogram depicting the compounds present in acai oil extracted from freeze-dried acai berry

The peaks in figure 6 display the nonpolar components of the acai oil. The following peaks were identified as follows: Hi-oleic safflower oil with retention at 3.200 min; 1-nitropiperidine with retention at 7.542 min; 1-dodecyn-4-ol with retention at 8.333 min; 2-heptenal with retention at 8.517 min; octanol with retention at 9.267 min; caprylene with retention at 9.967 min; 2-octenal with retention at 10.158 min; nonanal with retention at 10.825 min; oleic acid with retention at 12.633 min; 2-tridecenal with

retention at 12.850 min; 2-decenal with retention at 13.050 min; 2,4-decadienal with retention at 13.483 min; 2,4-dodecandienal with retention at 13.792 min; docosane with retention at 17.564 min; 1,4,6,9-nonadecatetraene with retention at 16.433 min; α-ketosteric acid with retention at 18.899 min; docosane isomer with retention at 19.158 min; docosanoic acid with retention at 20.458 min; 2-hexenyl-benzoate with retention at 21.917 min; 8,11,14 – eicosatrienoic acid with retention at 22.750 min; pantalene with retention at 23.889 min; eicosane with retention at 25.012 min; nonadecane with retention at 24.308 min; farnesol with retention at 24.657 min; isochapin B with retention at 25.233 min; heptaeicosane with retention at 25.801 min; farnesol isomer with retention at 27.042 min.

Acai oil was obtained initially from the acai berry Amazon juice blend that was purchased from Lakewood until the freeze-dried berry was obtained. For comparison, oil from the juice blend was extracted and analyzed under the same GC/MS conditions as the oil obtained from the acai berry. There were similar compounds found in the oil obtained from the berry, though not as abundant.

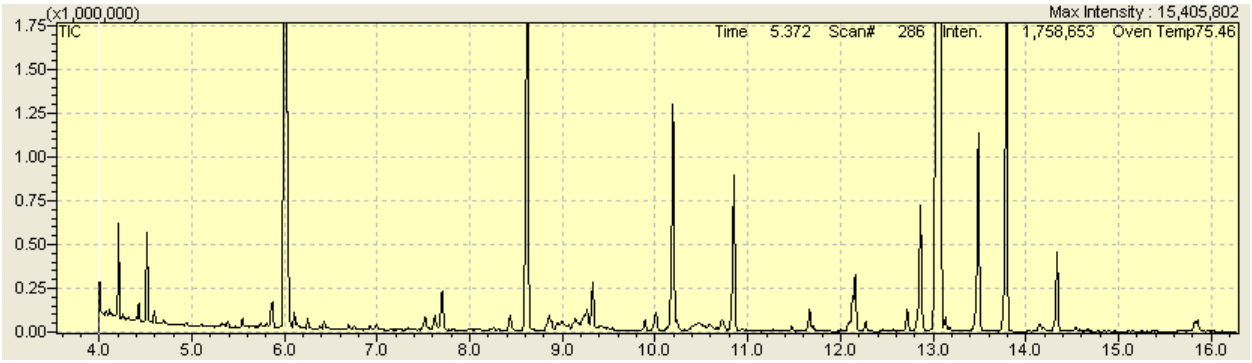

Figure 8 Chromatogram showing peaks corresponding to the aldehydes present in acai oil from 4 – 16 minutes

The chromatograph in figure 8 shows compounds present in the oil extracted from the pulp of the acai juice blend. The total run time for this chromatogram was 25 minutes as there were no peaks eluting from the column past 16.5 minutes. It is clearly obvious that the chromatograms for oil extracted from natural, unprocessed acai berry and acai juice blend are different. The peaks correspond to the following compounds: Ethyl formate with retention at 4.435 min; butanal at 4.551 min; octane at 6.05 min; heptanal at 7.785 min; 2-heptanal at 8.589 min; octanal at 9.323 min; 3-octen-2-one at 10.01 min; 2-octenal at 10.112 min; nonanal at 10.899 min; 2-nonenal at 11.876 min; 3-tridecene at 12.115 min; 2-decenal at 12.900 min; 2-undecenal at 14.872 min.

Many of the components of the acai oil are potential inhibitors for cytochrome P450s. For example, aldehydes are a well-known group of organic compounds that inhibit P450s. A study from the University of Michigan used primary, secondary and tertiary aldehydes in P450 assays and found that according to their K_{inact} values, primary

aldehydes showed greater inhibition than secondary and tertiary (39). From the GC chromatograms generated about 45% of the components in the acai oil are primary aldehydes, which suggest that the acai oil and one or several of its aldehyde constituents may have inhibitory properties toward certain cytochrome P450 enzymes.

3.2.0 Quantitative Data and Michaelis-Menton Kinetics

3.2.1 CYP_{2E1} Kinetics and Inhibition

Our initial study focused on CYP_{2E1}, an isoform that becomes induced upon the consumption of ethanol. This enzyme is important in human toxicology due to its role in carcinogen activation and potential to cause oxidative stress as discussed in the introduction. In order to establish an active inhibitor concentration for CYP_{2E1} an initial screening was done in duplicate (Figure 9) where varying concentrations of acai oil (1.6 μg/mL - 32 μg/mL) were incubated at 37°C for 30 minutes as previously described. Based on the results of the screening assay, the 32 μg/mL concentration was used to fully characterize CYP_{2E1} inhibition, since this concentration of oil gave roughly a fifty percent decrease in enzyme activity.

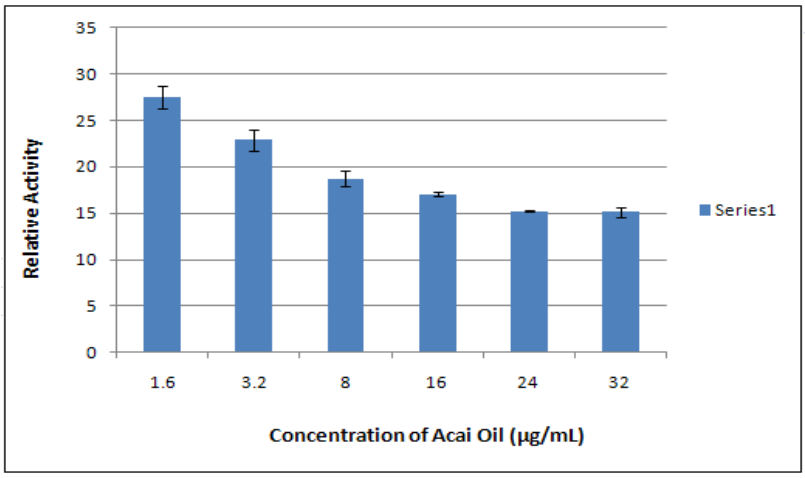

Figure 9. Dose-dependent screening for determining oil concentrations for CYP_{2E1}

Figure 8 shows the varying concentration of acai oil used in the screening assay along the x-axis and the y-axis displays the relative activity of 2E1 from the reaction. A sample chromatogram showing nitrophenol and nitrocatechol peaks are shown in Figure 10. The peak at 2.5 min was integrated and this area was used to monitor the relative activity of the enzyme. The graph shows that increasing the amount of acai oil results in a decrease in CYP_{2E1} activity, showing close to fifty-percent decrease in 2E1 response at 32µg/mL. This suggests that the IC_{50} for the acai oil for this P450 is around 30µg/mL.

Once the most potent concentration of acai was established, the P450 assay was conducted using the method described in section 2.3.1. Data was plotted as a Michaelis-Menton curve using SlideWrite data-processing software where the line of best fit was adjusted to fit Equation 3.1. Figure 11 displays the Michaelis-Menton curve generated using p-nitrophenol concentrations ranging from 4 – 32 µM in the absence and presence

of 32 µg/mL acai berry oil. The relative activity is recorded in arbitrary absorbance units based on the integration of HPLC data as previously described.

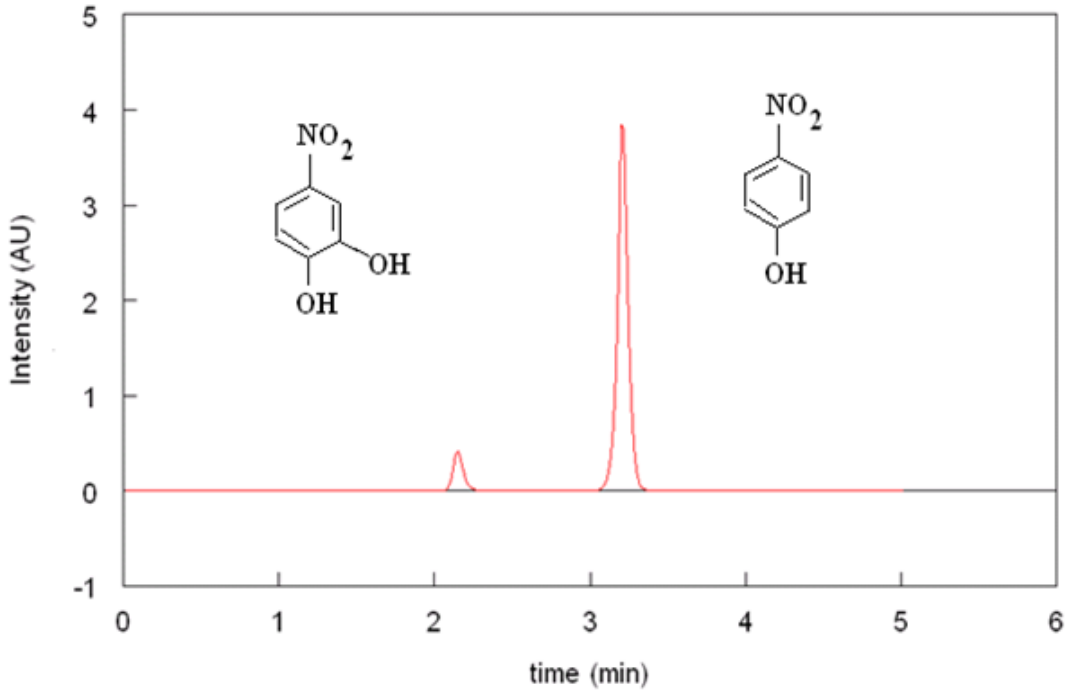

Figure 10. Chromatogram depicting the elution times for p-nitrocatechol (t_R = 2.51 min) and p-nitrophenol (t_R = 3.309 min)

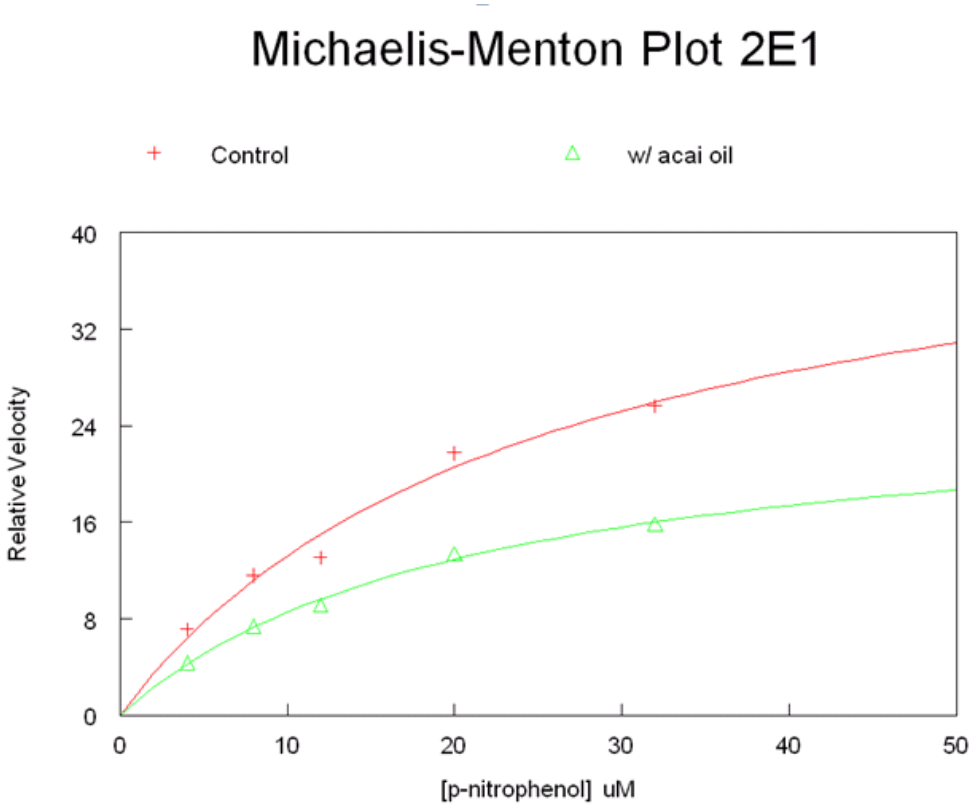

Figure 11 Michaelis-Menton plot showing relative velocities for CYP_{2E1} using 32 µg/mL acai oil

Because this study looks at inhibition, we used relative velocity to describe the rate of the reaction. Here, the relative velocity is defined as the change in the product's peak intensity over a 30 minute reaction time period. As all enzyme concentrations and reaction times were identical, the relative velocity units can be simplified to absorbance units correlating to the peak area for the product peak in the HPLC experiment. The data showed that the maximum velocity, V_{max}, was significantly lowered when the reactions were carried out in the presence of the acai oil. The following saturation equation, also known as the Michaelis-Menton equation, is used to determine the substrate

concentration at the initial kinetic rate where the variable V_{max} can be extrapolated from the saturation curve as shown in figure 11. The variable K_m, defined as the concentration of the substrate at half the maximum velocity, can be obtained by fitting the data obtained in the experiments using the mathematical relationships below (24).

$$v_0 = \frac{V_{max}[S]}{K_m + [S]}$$

Equation 2. Expression of relative velocity as the ratio of V_{max} as a function of substrate concentration

$$v_0^{-1} = \frac{K_m + [S]}{V_{max}[S]} = \frac{K_m}{V_{max}[S]} + \frac{1}{V_{max}}$$

Equation 3. Representation of Lineweaver-Burke data using reciprocal values to determine V_{max} and K_m

From the Michaelis-Menton data we see that the relative velocity of the reaction was decreased with little or no change in K_M; this behavior is indicative of pure non-competitive inhibition. This inhibition type occurs when the inhibitor binds to the free enzyme (E) and the enzyme substrate complex (ES) with similar affinities, implying that thte inhibitor binds to an allosteric regulator site rather than in the active site (23, 24). Equation 3 is the inverse relation of Equation 2, known as a Lineweaver-Burke relationship which allows the determination for the maximum velocity and K_m value

using linear regression (24). It allows for a visible inspection of the mode of inhibition without non-linear regression analysis. From the Michaelis-Menton plot V_{max} and V_{max}^{app} values were estimated to be 34 and 18 (arbitrary units) respectively, showing that there was a fifty-percent decrease in the reaction rate in the presence of the acai oil. Here V_{Max}^{app} is defined as V_{Max} in the presence of inhibitor. A determination of values of K_M and K_M^{app} were determined from the generated Lineweaver-Burke plot (Figure 12). The values for K_M can be obtained from the linear function generated by the SlideWrite software by taking the negative-inverse of the x-intercept values; thus, the value for K_M was found to be 12.5 µM and 20 µM for K_M^{app} . Because K_M and K_M^{app} were within 15% of each other, this suggests nearly pure non-competitive inhibition, indicating that the inhibitor (I) binds to E and ES with nearly the same affinity (24).

The concentration of oil necessary to induce inhibition is established by the constant K_I which is defined as the ratio of inhibitor concentration and the difference in the correction factor α by a magnitude of one (Equation 5). The term α is expressed as a ratio between K_m and K_m^{app} (Equation 4). The derivation of equation 5 allows us to calculate the K_I directly given the known values for each of the constants. The value for α can also be obtained directly from the slope corresponding to the linear functions generated from the Lineweaver-Burke plots (m = 2.261 for wildtype and m = 3.767 for data with inhibitor).

$$\alpha = \frac{V_{Max}}{V_{Max}^{app}}$$

Equation 4. Expression of the correction factor α as a ratio of the maximum velocities

$$\alpha = 1 + \frac{[inhibitor]}{[K_I]}$$

$$[K_I] = \frac{[inhibitor]}{\alpha - 1}$$

Equation 5. Derivation of K_I using known values for inhibitor concentration and α

The dissociation constant for the inhibitor, K_I, is a measure of the separation inhibitor from the P450. It is the concentration of inhibitor required to decrease the maximal rate of the reaction to half of the uninhibited value (23). Using equation 4 the calculated value for the correction factor α was determined to be 1.89; this value is consistent with the constraint that the value of α must be greater than 1(24). Thus, the concentration of acai oil needed to lower the maximal velocity of 2E1 is 36 μg/mL.

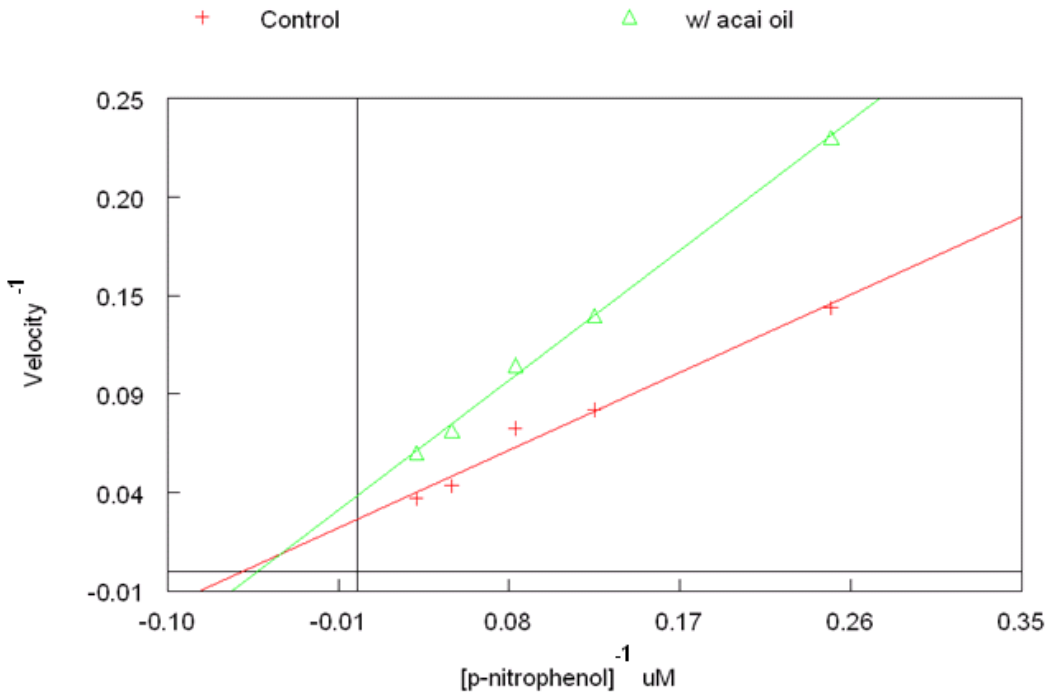

Figure 12. Lineweaver-Burke plot depicting mixed-type inhibition for CYP_{2E1}.

From the Lineweaver-Burke plot provided it is evident that the two data sets, the control with no inhibitor and the data obtained in the presence of inhibitor, intersect at slightly above the x-axis suggesting that the inhibition type is purely non-competitive. Characteristics associated with non-competitive inhibition are that the inhibitor binds directly to an alternative or allosteric site which directly alters enzymatic activity, which manifests as a significant lowering of the maximum velocity as shown from the Michaelis-Menton curve (24).

The catalytic rate, denoted as k_{cat}, is a measure of the catalytic efficiency for the conversion of p-nitrophenol to p-nitrocatechol per unit of time. The value for k_{cat} can be

obtained from the ratio of the maximum velocities and the concentration of enzyme (24). Since the microsomes used in all P450 assays did not contain pure isoforms the k_{cat} for all CYP analyses could not be determined since the actual concentration of 2E1, 2A6 or 2B4 could not be determined.

3.2.2 CYP_{2A6} Kinetics and Inhibition

An important isoform of the P450s is the subfamily CYP_{2A6}, which is well known for metabolizing xenobiotics and commercial pesticides consumed from fresh produce. It is the most important P450 that is responsible for the metabolism of nicotine and cotinine, two compounds found in tobacco. CYP_{2A6} is also reknown for its ability to activate nitrosamines - components found in tobacco products that enter the bloodstream upon inhalation via primary or secondary smoking that are known carcinogens (12). CYP_{2A6} is the enzyme involved in nicotine metabolism, converting nicotine into cotinine while at the same time activating procarcinogens present in tobacco; thus, it has received interest as a possible target for smoking cessation therapy (40). Furthermore, studies reveal that various medications are known to induce and suppress CYP_{2A6} activity, among them include selective serotonin re-uptake inhibitors (SSRIs) that inhibit 2A6 activity and dextromethorphan, a drug that has been shown to induce 2A6 activity (40).

The substrate used to probe inhibition for this isoform was coumarin, a well known drug used to regulate edema (13). It is found in many plant species, with the

tonka bean (*Dipteryx odorata*) containing the highest concentrations. It is metabolized naturally by most fungi to 4-hydroxy coumarin, which is used in pharmaceuticals as an anticoagulation agent (13). For the purpose of this study, the hydroxylation of coumarin at the C-7 position indicates that this reaction is specific for 2A6, since microsomes consist of a mixture of many different P450s.

The determination of substrate concentration and acai oil was performed as an initial screening assay, similar to the screening methodology for CYP_{2E1}. The graph in Figure 13 represents the screening for CYP_{2A6} using a concentration range of 10.4 µg/mL – 208 µg/mL range for the inhibitor. The data in Figure 13 reveals an unusual increase in enzyme activity at acai oil concentrations greater than 50 µg/mL. The screening was repeated three consecutive times, resulting in the same trend as shown. A hypothetical explanation for this trend leaned on the idea that there exists a compound or set of compounds in the acai oil that interferes with the reaction mechanism for 2A6, and potentially a subset of compounds that may stimulate P450 activity.

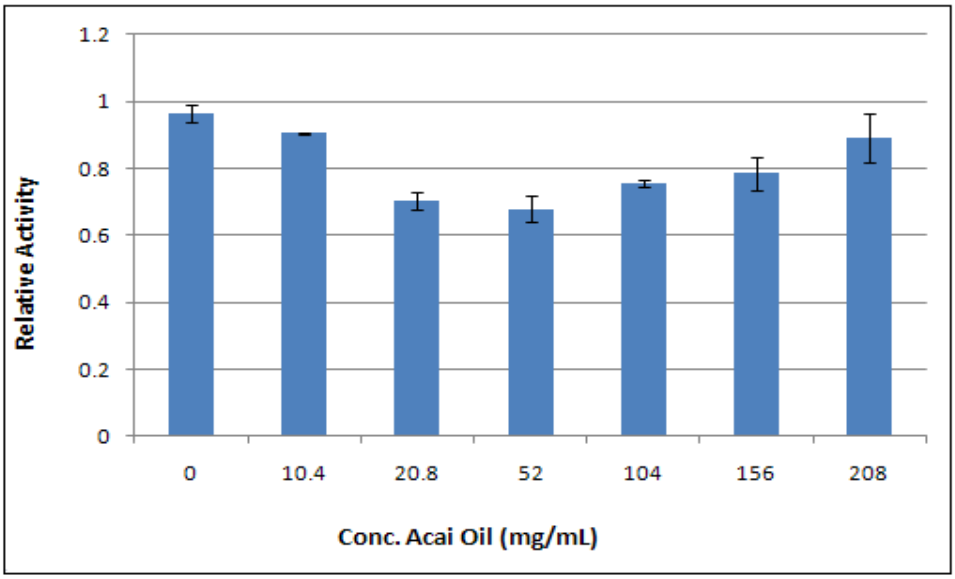

Figure 13. Screening for CYP_{2A6} for potency using increasing concentrations of acai oil

The initial screening suggests that this unusual trend in activity results in maximum inhibition; therefore, 52 µg/mL acai oil was used in the subsequent kinetic analysis of 2A6 using the Michaelis-Menton model.

Figure 14 below shows the Michaelis-Menton plot for a 2A6 assay consisting of a control and a reaction containing 52 µg/mL acai oil. A previous 2A6 assay using 25 µL of acai oil solution showed minimal decrease in relative velocity; thus, it was determined that around 50 µg/mL showed the most significant effect on the reaction kinetics. From the data in figure 14, the maximum relative velocity for the control was estimated using raw data as shown. There is a significant decrease in relative velocity and very little or no change in the value of K_M, suggesting pure, non-competitive inhibition. As previously stated, the actual values for K_M and V_{Max} can be calculated from the Lineweaver-Burke

plots for the control and the reaction data that was observed in the presence of the acai oil (see Figure 15).

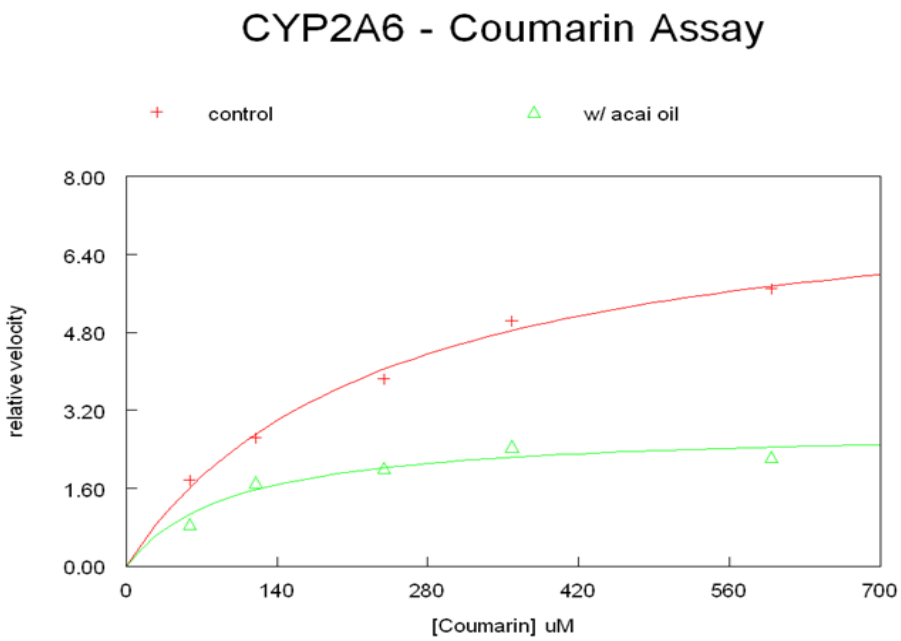

Figure 14 Michaelis-Menton plot for CYP_{2A6} showing a decrease in V_{Max} upon incubating with 52 µg/mL acai oil

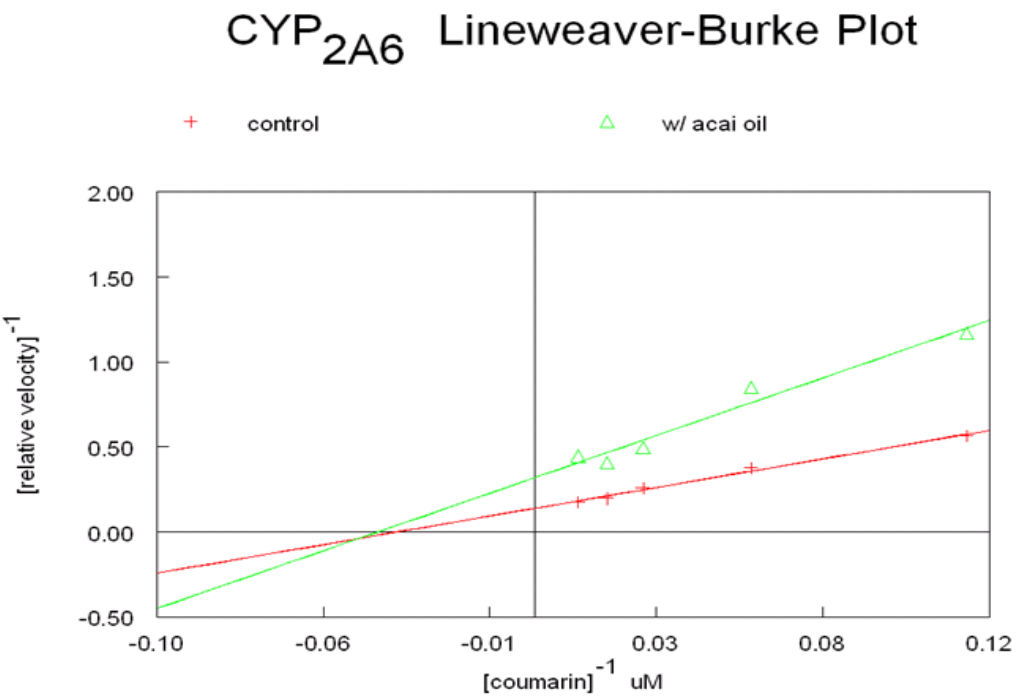

Figure 15. Lineweaver-Burke plot for CYP_{2A6}.

The calculated maximum velocity for the control, V_{Max}, was determined to be 7.16 and 3.13 for the maximum velocity regarding the data containing the inhibitor, V'_{Max}. The Michaelis constants, K_M and K_M^{app}, were found to be 27.39 µM and 24.09 µM respectively. Referring to the Lineweaver-Burke plot, the correction factor α for non-competitive inhibition is defined as the ratio of the slope for each linear function. The corresponding values for α and α′ were 3.8233 and 0.4963 respectively. Using equation 4 we can determine the value for K_I by rearranging the equation and obtain equation 5 which allows us to calculate the value for K_I which was determined to be 19.48µg/mL.

It is curious that both isoforms appear to be inhibited via pure non-competitive type inhibition. A proposed mechanism that could be responsible for the large decreases in V_{Max} is that the compounds in the acai oil could potentially be interfering with the CPR system. A more direct hypothesis is that the acai oil could be interfering with the FAD cofactor, which is responsible for the influx of electrons into the P450. If the supply of electrons is altered which ultimately leads to an inefficient reduction for the iron-oxo heme moiety, then a general reduction in the observed V_{Max} may be expected for all P450s. The oil may also interfere with the formation of the P450-reductase complex that must transiently form in the course of transferring electrons.

3.2.3 CYP_{2B4} Kinetics

The last isoform that was probed in this study was CYP_{2B4} which is associated with the oxidation of high molecular weight, aromatic substrates. Metabolic studies using rats and rabbit P450s showed that CYP_{2B4} is induced by the psychomimetic drug Phenobarbital: It acts to either oxidize or reduce the substrate that binds to it while at the same time utilizes molecular oxygen to initiate a free radical mechanism in the formation of the product (6). There are two assays used to probe for activity: The Nash assay, which utilizes the Nash reagent (chemical composition discussed in Section 2.1.5) to monitor the formation of formaldehyde using basic UV absorption spectroscopy: The use of benzyl alcohol to monitor the formation of benzaldehyde using reverse-phased HPLC. In the former reaction the substrate N, N-dimethylaniline is demethylated to produce N-methylaniline and formaldehyde: The reaction of formaldehyde with the Nash reagent

produces a color change after incubation. This colormetric method was used to quantify the formaldehyde produced from the reaction of N, N-dimethylaniline with 2B4. The results of this study suggested a slight increase in catalytic activity in the presence of the oil. Because the assay uses a non-specific spectrophotometric approach to quantify the product, it was unclear whether true activation of the enzyme was occurring or whether compounds in the oil interfered with the colormetric analysis. Therefore, a second assay was employed in which benzyl alcohol was oxidized to benzaldehyde with HPLC detection.

Both of these assays are quantitative but utilize different reagents and incubations. The overall reaction for the assays shown in Figure 16 below depicts the formation of N-methylaniline and formaldehyde in the Nash assay and the oxidation of benzyl alcohol to benzaldehyde for the HPLC method.

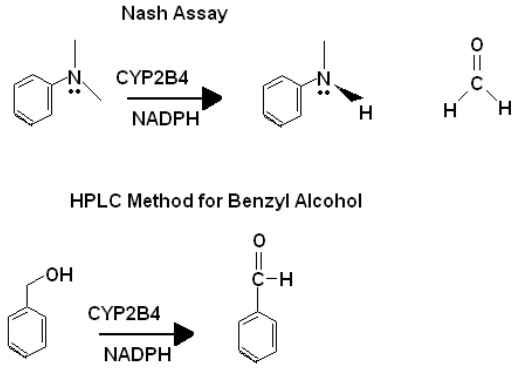

Figure 16. Reactions for probing CYP_{2B4} monitoring the reaction of formaldehyde with the Nash reagent (top) and monitoring the formation of benzaldehyde from benzyl alcohol (bottom)

The data generated from the CYP_{2B4} assays did not indicate acai oil had a significant effect on CYP_{2B4} activity, as there was little to no effect on the maximum velocity. As previously mentioned, the two methods used to probe CYP_{2B4} both generated data that suggests no activity using acai berry oil. The reaction procedure was repeated several times showing the same trend where no activity was observed. In fact, a reproducible slight increase in the apparent activity was observed in the experiments involving dimethylaniline. Figure 17 shows the Michaelis-Menton plot from the data obtained from a Nash assay; it clearly depicts an increase in V_{Max}^{app} suggesting that the components in the oil compete with formaldehyde with N-methylaniline or one of the compounds in the oil directly stimulates 2B4 at an allosteric site which directly contributes to an increase in signal. Because of the presence of aldehydes in the acai oil an alternative assay was used to rule out the possibility that acai was not a potential inhibitor at all, but rather the Nash reagent simply reacted with the aldehydes present in the oil to give a positive signal.

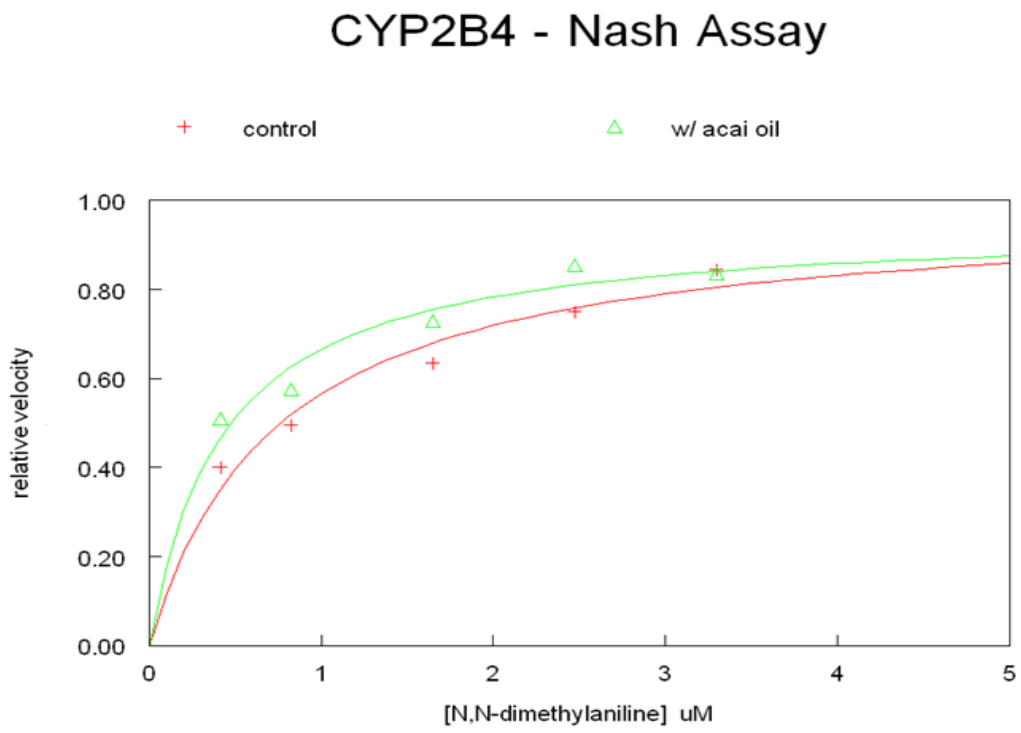

Figure 17. Michaelis-Menton plot for CYP_{2B4} where interference of signal is observed by an increase in V_{Max}^{app}

The alternative method utilized reversed-phase chromatography to separate benzaldehyde, the metabolite from benzyl alcohol oxidation. Following the reaction with CYP_{2B4} at 37°C using the same reaction procedure discussed in Section 2.1.6, there was initially an insignificant amount of benzaldehyde produced in the reaction. Increasing benzyl alcohol concentrations to 50 – 400 µM resulted in observable benzaldehyde peaks in the chromatogram (Figure 19). Once control activities were observed, various aliquots of acai oil were used to probe CYP_{2B4} for alterations in activity using a concentration range from 4.16 – 20.8µg/mL acai oil.

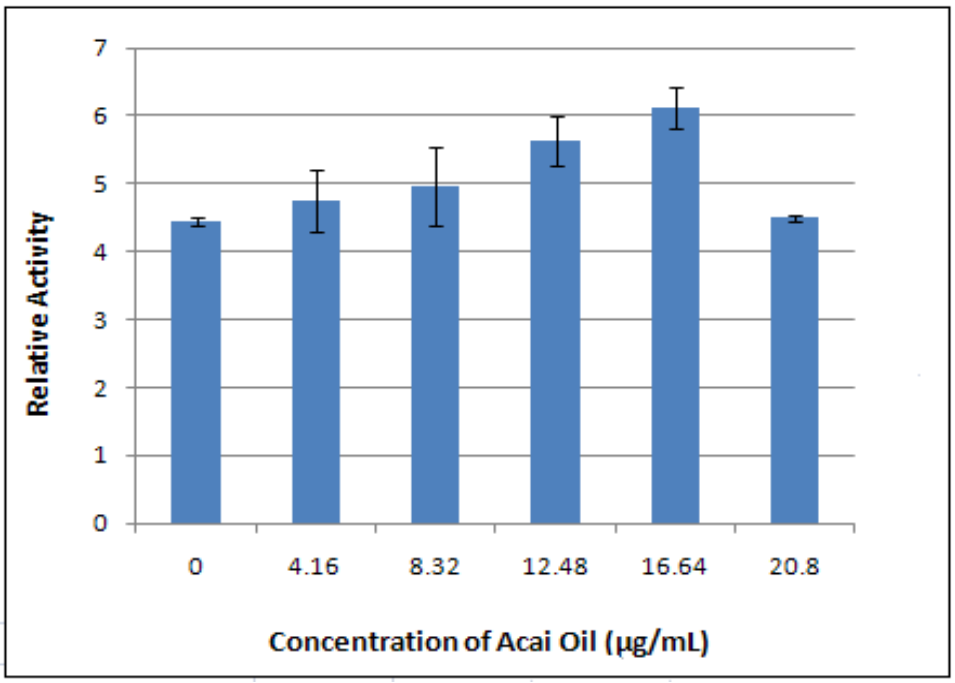

Figure 18. Initial screening for CYP_{2B4} showing a significant increase in relative activity upon exposure to acai oil between 12-16 µg/mL concentrations

The initial screening assay consisted of six reaction tubes with enzyme, buffer, water, 65µL of 1.2 mM benzyl alcohol along with the varying concentrations of acai oil. Upon HPLC analysis the signal generated was used to quantify the amount of benzaldehyde produced from the reactions. The 2B4 chromatogram in Figure 19 below depicts the amount of benzaldehyde formed from the reaction compared to the amount of benzyl alcohol, where integration of the benzaldehyde peak at 1.590 minutes was used to monitor the overall activity in the reaction assay.

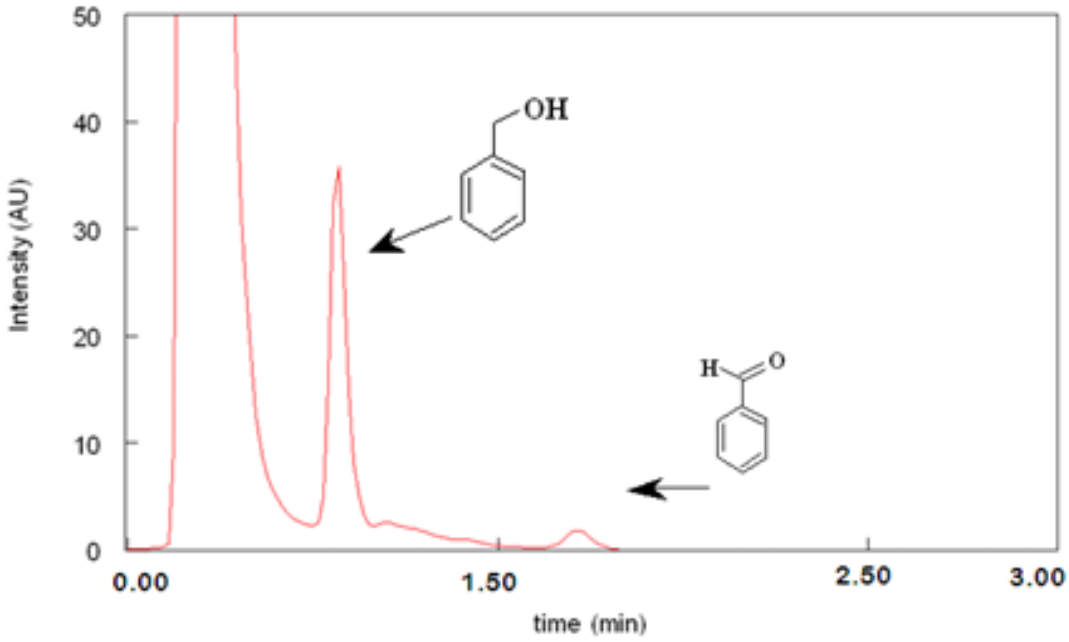

Figure 19. Chromatogram depicting the retention times for benzyl alcohol and benzaldehyde

The screening results suggest that acai oil stimulates enzyme activity at an average concentration of less than 17 µg/mL, though, higher oil concentrations showed that activity decreased at 20 µg/mL. Since the screening was carried out at a relatively high substrate concentration a kinetic analysis was performed in which the highest concentration was selected and substrate concentration was varied. The corresponding data is shown in Figure 20 in the double reciprocal plot. The curves suggest a modest increase in K_M and a slight decrease in V_{Max}; however, the observed changes are very modest and appear to fall within the error range. Thus, 20 µg/mL acai oil was used to probe inhibition using the Michaelis-Menton approach. A total of five reaction assays were performed using the reaction conditions and HPLC conditions previously described in Section 2.3.1. There was no significant change in maximum velocity for CYP_{2B4} or in

the observed K_M using 20 µg/mL acai oil. The V_{max} for the control and in the presence of inhibitor were almost identical. From the Michaelis-Menton plot (not shown) the V'_{Max} could not be determined because no saturation occurred for the data possessing the inhibitor. This behavior was observed for all five assay runs under the same experimental conditions. Figure 18 below shows the Lineweaver-Burke data for 2B4 where the location where the two functions intersect occur in quadrant I on the coordinate axis. Based on Michaelis-Menton kinetics the two functions must intersect at or below the x-axis corresponding to quadrant III. Therefore, the type of inhibition cannot be determined as the plot clearly shows that there is an increase in V_{Max} and V'_{Max}.

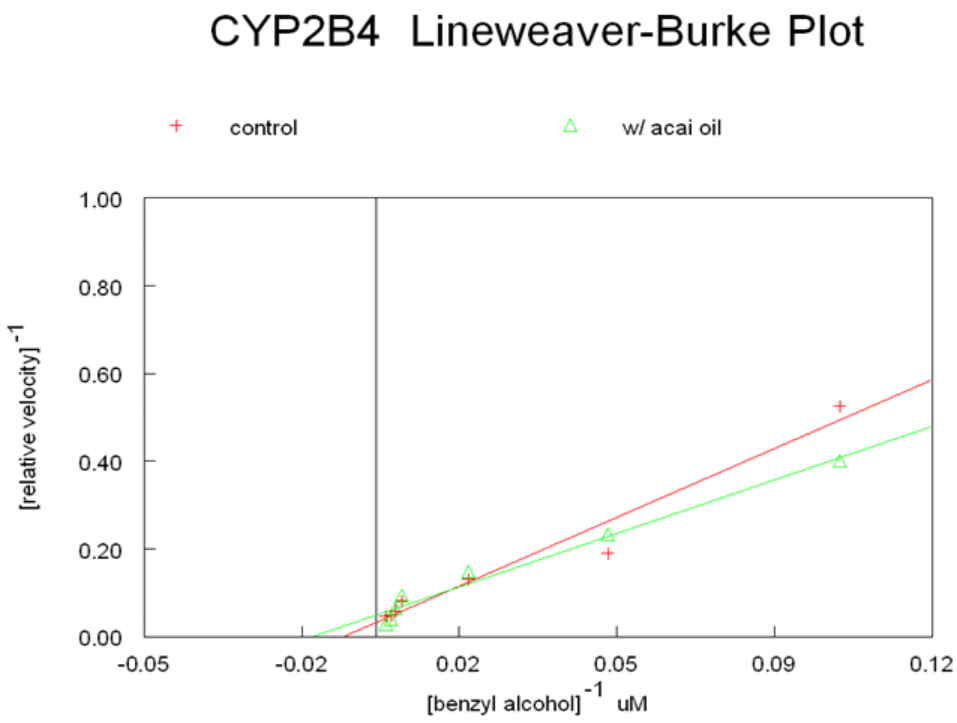

Figure 20 Lineweaver-Burke plot for analysis of benzaldehyde indicating saturation between 50 – 400 μM benzyl alcohol

From the Michaelis-Menton plot the maximum relative velocity for the control was estimated to be 23.9, but the reaction that contained the acai oil gave values that gave a broad stretch leaving no determination for V_{max}app. Based on the screening and the raw data, no conclusions pertaining to CYP_{2B4} can be made; thus, it appears that no interaction with 2B4 is likely to occur. This conclusion does suggest that the hypothesis stated earlier regarding the inhibition of P450 reductase by acai oil is not likely to be correct. As all P450s utilize the same reductase, one would expect inhibition of the reductase to cause a universal decrease in P450 activity. This does not seem to be the case based on the data for 2B4.

3.2.4 Monitoring Activity Using Acai Juice. As previously mentioned in section 2.4, acai berry juice was analyzed for its ability to decrease or inhibit cytochrome P450 activity. The juice was purchased from a local food store and was certified to be 100% organic, though it was found adulterated with other fruit juices. The purpose of this aspect of the research project served to observe similar activity as seen with the acai oil, suggesting that the acai berry juice blend contains similar ingredients that have the same inhibitory properties as the pure acai oil. The CYP_{2E1} isoform was used to probe for activity using acai juice.

As with the previous studies involving the oil, an initial screening was performed using the acai berry juice. It was determined based on the observation that a 25 µL aliquot caused a significant reduction in P450 activity the most significant activity was observed using 25µL of the juice. A series of experiments were conducted using 25µL of microsomes, 50 mM phosphate buffer, a range of 20 – 160 µM of p-nitrophenol, 1mM NADPH, and a 25µL aliquot of the acai juice blend in order to determine the mode of inhibition via Michaelis-Menton kinetic analysis. The concentration of the acai juice was determined by weighing 1mL of the acai juice to obtain the juice density, where corresponding aliquots of juice (5, 10, 25, and 50 µL) were factored into the total reaction volume (0.5mL) to obtain the concentrations listed in Figure 21 below.

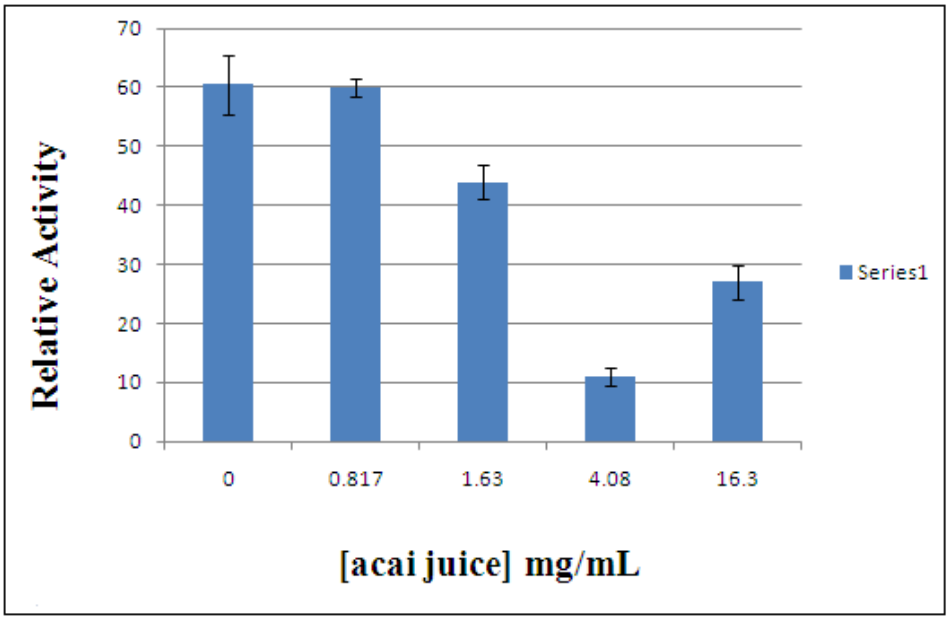

Figure 21. Screening of CYP_{2E1} incubated in the presence of increasing concentrations of juice

The screening assay for the acai juice showed a significant decrease in 2E1 activity at 4.08 mg/mL concentration. This finding is similar to the decrease in activity seen in the acai oil screening, suggesting that 2E1 either undergoes irreversible inhibition or mixed inhibition by some unknown mechanism.

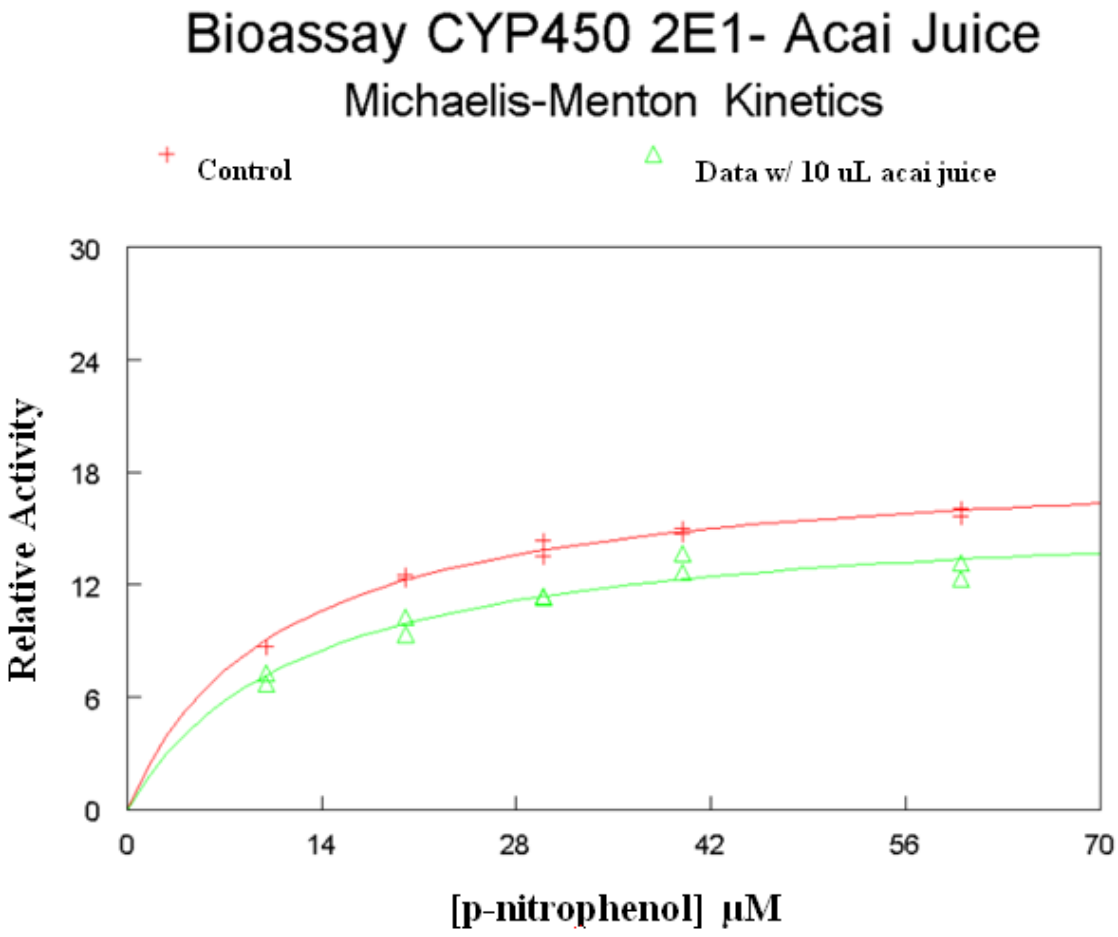

Figure 22. Michaelis-Menton plot illustrating the reaction kinetics for CYP_{2E1} in the presence of 10 µL acai berry juice

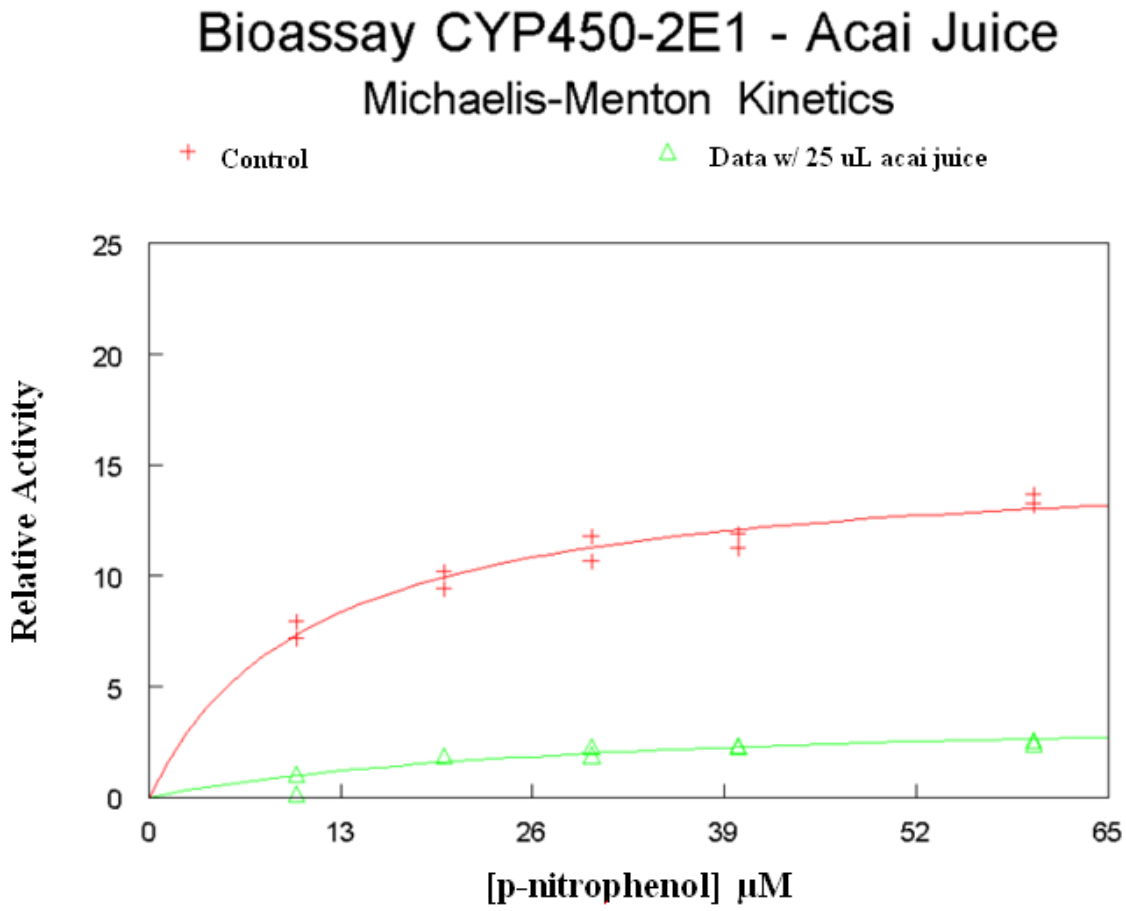

(B)

Figure 23. Michaelis-Menton plot for CYP_{2E1} incubated in the presence of 25 µL acai berry juice

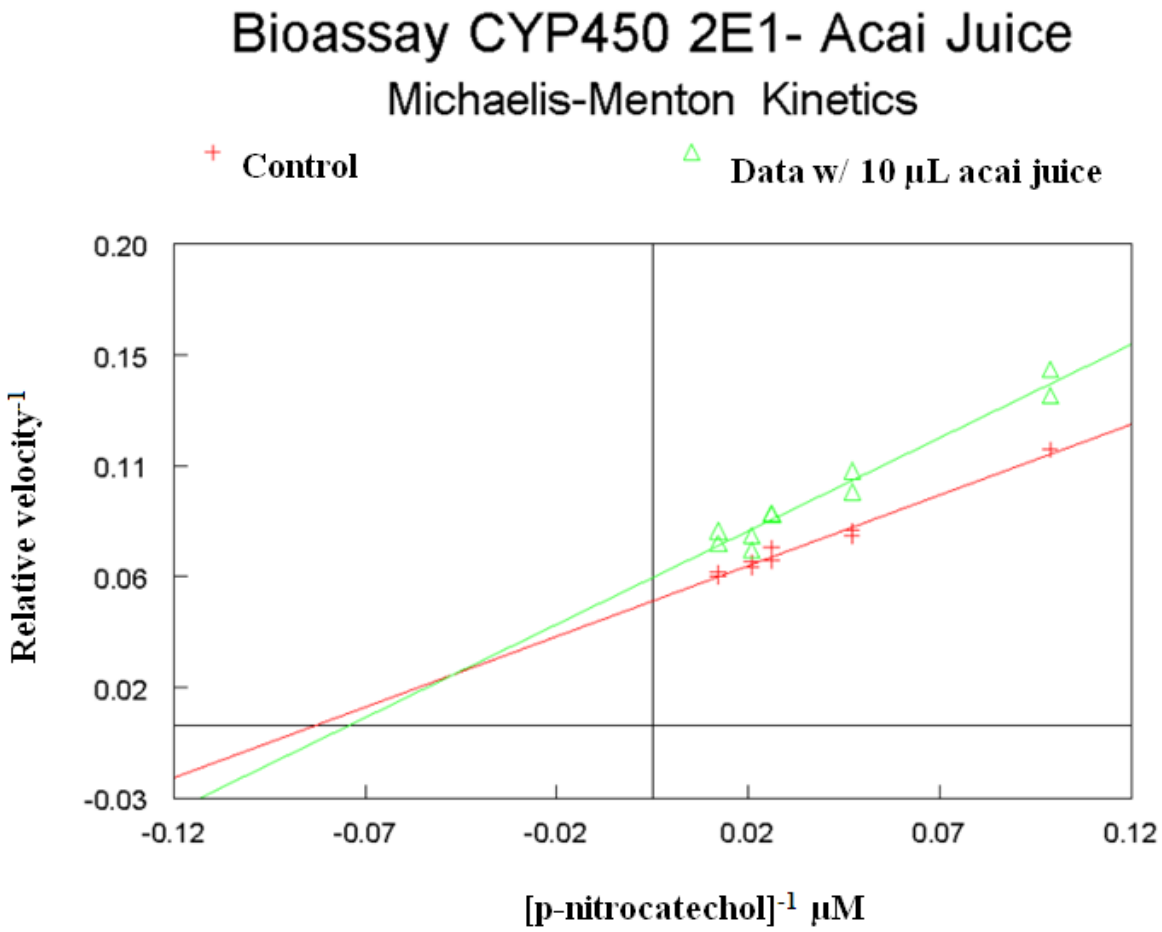

Figure 24. Lineweaver-Burke plot corresponding to the data where 10 µL acai berry juice was used as inhibitor

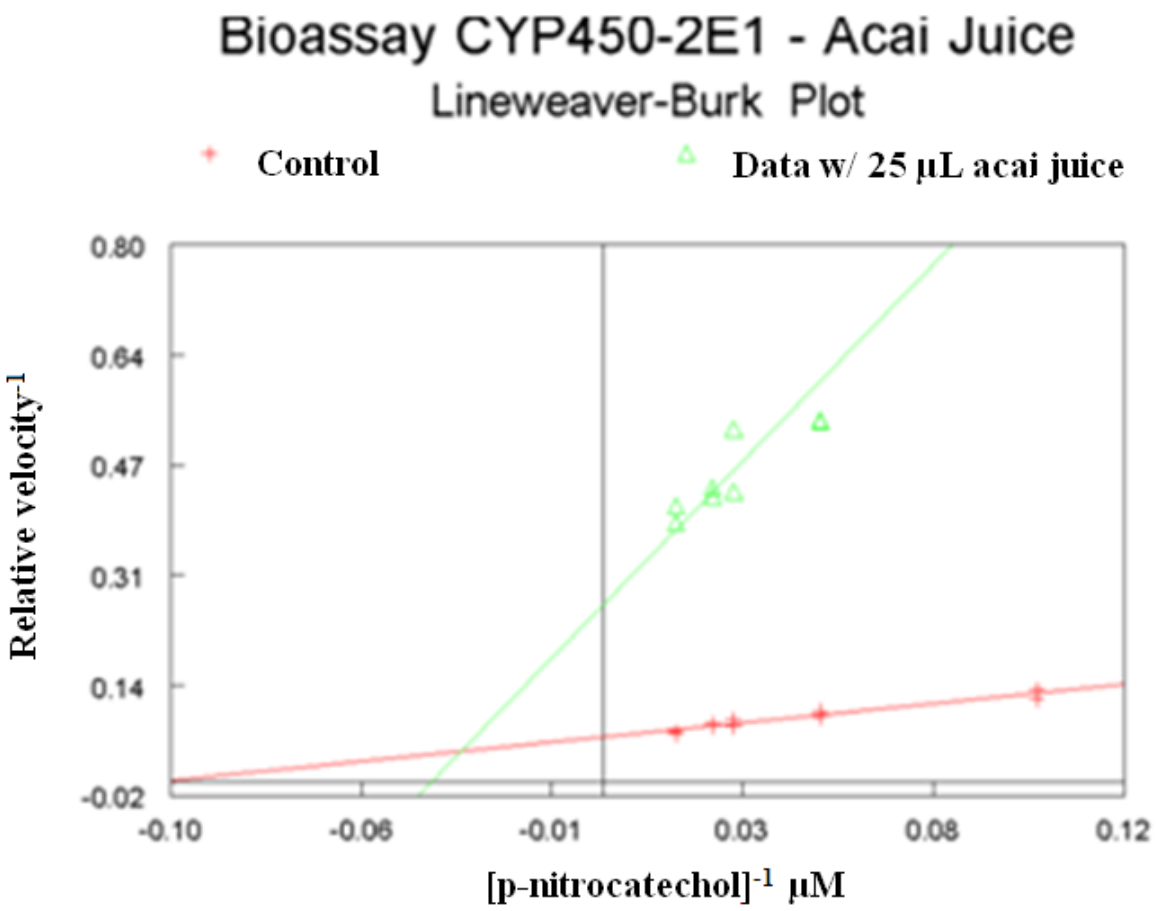

(B)

Figure 25. Lineweaver-Burke plot corresponding to the data where 25 µL acai berry juice was used as inhibitor

A second CYP_{2E1} assay was conducted using a 10µL aliquot of the juice blend. Figures 21 and 22 compare the relative activities using the two volumes. There is a significant decrease in reaction rate, corresponding to a 25-fold decrease in relative velocity, using 25µL compared to the assay that used 10µL of acai juice blend. The values for V_{Max} and V_{Max}^{app} regarding the assay where 10 µL was used were calculated to

be 18.5 and 16.95 respectively with values for K_m 11.36 µM and 12.82 µM for $K_m$app. However, there is a significant difference in the binding affinities when 25µL of acai juice blend is used in the assay. There is a large difference in the relative velocities where VMax and VMaxapp were found to be 12.50 and 3.57 respectively when 25 µL acai juice was used. The values for K_M and K_M^{app} were 6.67 mM and 20 mM respectively. In this experiment, V_{Max} and K_M are both altered in the presence of the juice, which indicates a mixed form of inhibition. This could be the result of the presence of multiple compounds in the juice with inhibitory properties. Clearly the interaction between CYP_{2E1} and the juice is somewhat different than that observed in the oil based on the altered Michaelis-Menton behavior observed. Another possibility for the mode of activity shown is irreversible inhibition. Aldehydes, haloalkanes and alkenes are known irreversible inhibitors for P450s. The functional groups associated with these compounds may form covalent adducts with the amino acid side chains or the heme group itself, altering the kinetic properties of the enzyme (15).

CHAPTER IV

CONCLUSION

This research investigated the properties of a naturally occurring fruit which is marketed as a supplement that is claimed to have very high anti-oxidant and energy-revitalizing effects from those that market acai and the natives from the South American region. From a metabolic standpoint, the findings of the current study suggest that there could be some degree of antioxidant properties of acai by virtue of its ability to block 2E1 activity. The qualitative investigation, all done by GC-MS, supports the claims that acai is high in phytochemicals that may be anti-oxidant in nature. Futhermore, the oil from the acai berry also contains compounds that act non-competitively to block both CYP_{2E1} and CYP_{2A6}.

Terpenoids and essential compounds such as oleic acid, which were identified from the TIC previously shown, are known compounds that induce P450 inhibtion as well as the numerous aldehydes present. Cinnamaldehyde, the main constituent from cinnamon which was screened along with other aldehydes, showed significant inhibition for CYP_{2E1}, suggesting that the majority of aldehydes found from natural sources are effective P450 inhibitors (33).

The enzyme kinetic assays used to test acai oil showed that for CYP_{2E1} and CYP_{2A6} the catalytic efficiencies were indicative of the lowering of the maximum velocity when probing for inhibition. The Lineweaver-Burke plots from both assays using the acai juice and the acai oil clearly demonstrated the type of inhibition observed for the two isoforms, which suggests non-competitive inhibiton. This tells us that the inhibition may occur at an allosteric site or binds directly to the active site on the P450 enzyme. CYP2E1 is known to possess an effector site which may be involved where high concentrations of p-nitrophenol bind to the effector site, slowing the rate of catalysis. Another possibility to support this idea is that an additional p-nitrophenol or an aldehyde present in the acai oil binds to the effector site and slows the release of product, reducing the overall rate of catalysis.

The most potent activity that occurred between the two isoforms was for CYP_{2A6} where the K_I for acai was determined to be 5.5µg/mL. Incubating CYP_{2A6} at higher concentrations of oil seemed to raise activity, suggesting that the oil has no overall effect.

Regarding the CYP_{2B4} assay, it can be concluded that the signal obtained from the spectrophotometer was the result of one or more of the aldehydes naturally occurring in the oil, which interfered with the detection of formaldehyde. The GC chromatograms of the acai berry oil showed >55% aldehyde composition. It can be inferred that the lack of enzyme activity is directly related to the presence of various natural aldehydes present in the oil as previously mentioned in Section 2.3.1.

Comparing the oil assays with the juice blend assay it can be inferred that the acai juice blend, which contained other fruit juices, contains a large amount of compounds that are found in the acai oil based on both the GC-MS analysis and the quantitative data obtained to measure the decrease in enzyme activity. Furthermore, the juice blend shows some beneficial effects and can be used as a substitute for pure acai. Also, very little oil was extracted from the juice blend suggesting that the amount of non-polar components are not as abundant as found in naturally occurring acai berry.

The significance of these findings suggests acai is a beneficial fruit and dietary supplement. People taking prescription medications such as coumarin or medications used to treat fungal infections can safely take these drugs without worrying about drug interactions related to the fruit. The qualitative data shows that there are many terpenoids and other phytochemicals that can be used as precursors to engineer other drugs. Isolation of these high molecular weight compounds poses a challenge, though advance separation techniques could be implemented in order to see if any one of these compounds could show a significant lowering of P450. Since acai contains a large number of different compounds in the oil, juice and pulp there could be potentially a large number of individual compounds that strongly inhibit P450 activity. This research can be used as a precursor to explore different separation techniques in an attempt to measure inhibition or stimulation, or test the antioxidant properties of each individual compound.

REFERENCES

1. Meunier, B; de Visser, S.P; Shaik, S. **2004** *Chem Rev*., *104*, 3947 – 3980
2. Appendino, G.; Cravatto, G; Sterner, O; Ballero, M. **2001** *J. Nat. Prod.*, *64*, 393-395
3. Blobaum, A. L. *Drug Metab. Dispos*., **2006**, 34:1, 1
4. Yang, S; Wilson, K; Kawa, A; Raner, G.M. *Food Chem Toxicol*., **2006**, *44:7*, 1075-1077
5. Zhizhina, G.P; Blyukhterova, N.V. *Biochemistry*, **1996,** *62:1*, 88 – 94
6. Guengerich, F.P. *Chem. Res. Toxicol.*, **2008**, *21:1*, 70 – 83
7. Day, B. J; Kariya, C. *Toxicological Science*, **2005**, *85:1*, 713 – 719
8. Lu, A. Y.; Junk, K. W.; Coon, M. J. *J. Bio Chem*, **1969**, *244:13*, 3714 – 3721
9. Osawa, Y.; Pohl, L. R. *Chem. Res. Toxicol*, **1989**, *2:3*, 136
10. Shaik, S.; Kumar, D.; de Visser, S. P. *J. Am. Chem. Soc*., **2008**, *130*, 10128 – 10140
11. Sligar, S. G.; Cinti, D. L.; Gibson, G. G.; Schenkman, J. R. *Biochem. Biophys. Res. Commun.*, **1979**, *90:3*, 925 – 932
12. Auclair, K.; Hu, Z.; Little, D. M.; Ortiz de Montellano, P. R.; Groves, J. T. *J. Am. Chem. Soc.*, **2002**, *124*, 6020

13. Raner, G. M.; Hatchell, A. J.; Morton, P. E.; Ballou, D. P.; Coon, M. J. *J. Inorg. Biochem.*, **2000**, *81*, 153

14. Kuo, C. L.; Raner, G. M.; Vaz, A. D.; Coon, M. J. *Biochemistry*, **1999**, *38*, 10511

15. Meunier, B.; Bernadou, J. *Struct. Bonding*, **2000**, 97, 1

16. De Visser, S. P.; Shaik, S. J. *J. Am. Chem. Soc*., **2003**, *125*, 7413

17. Obach, R. S. *Drug Metab. Dispos*., **2001**, *29*, 1599

18. Reilly, C. A.; Ehlhardt, J.; Jackson, D. A.; Kalonthalvel, P.; Mutlib, A. E.; Espina, R. J.; Moody, D. E.; Crouch, D. J.; Yost, G. S. *Chem. Res. Toxicol*. **2003**, *16*, 336

19. Hukkanen, J; Jacob, P. *Clin. Pharmacol. Ther*., **2006**, *80:5*, 522 – 530

20. He, K.; Iyer, R.; Hayes, R. N.; Sinz, M. W.; Woolf, T. F.; Hollenberg, P. F. *Chem. Res. Toxicol.*, **1995**, *11:4*, 252 – 259

21. Yamazaki, H.; Johnson, W. W.; Ueng, Y. F.; Shimada, T.; Guengerich, F. P. *J. Biol. Chem*., **1996**, *271:44*, 27438 – 27444

22. Cornish-Bowden, A. *"Fundamentals of Enzyme Kinetics*", Butterworths Publishing, Portland, **1979**

23. Fersht, A. *"Enzyme Structure and Mechanism,"* Freeman Publishing, San Diego, **1985**

24. Voet, D., Voet, J., Pratt, C. *"Fundamentals of Biochemistry,"* Wiley, Seattle, **2004**

25. Zhou, S. *Clin. Pharm*., **2005**, *44:3*, 279 – 304

26. Ortiz de Montellano, P. R.; Stearns, R. A.; Langry, K. C. *Mol. Pharmacol*., **1984**, *25*, 310

27. Estabrook, R. W. *Drug Metabolism and Disposition*, **2003,** *31*, 1461 – 1473

28. Zhoupeng, Z.; Li, Y.; Stearns, R. A.; Ortiz de Montellano, P. R.; Bailhie, T. A.; Tang, W. *Biochemistry*, **2002**, *41*, 2712

29. Lieber, C. S. Hepatology, **1984**, *4*, 1243 – 1260

30. Moreno, R. L.; Kent, U. M.; Hodges, K.; Hollenberg, P. F. *Chem. Res. Toxicol*., **1999**, *12*, 582 – 587

31. Lee, J. H.; Johnson, J. V.; Talcott, S. T. *J. Agric. Food Chem*., **2005**, *53*, 6003 – 6010

32. Olsson, M. E.; Gustavsson, K. E.; Andersson, S. *J. Agric. Food Chem*., **2005**, *52*, 7264 – 7271

33. Singh, G.; Maurya, S.; de Lampasona, M. P.; Catalan, A. N. *Food and Chem. Toxicol*., **2005**, *45*, 1650 – 1661

34. Schauss, A. G.; Wu, X.; Prior, R. L.; Ou, B.; Huang, D.; Owens, J.; Agarwal, A.; Jensen, G. S.; Hart, A. N.; Shanbrom, E. *J. Agric. Food Chem*., **2006**, *54*, 8604 – 8610

35. Chin, Y. W.; Chai, H. B.; Keller, W. J.; Kinghorn, A. D. *J. Agric. Food Chem*., **2006**, *56*, 7759 – 7764

36. Mertens-Talcott, S. U.; Rios, J.; Jilma-Stohlawetz, P.; Pacheco-Palencia, L. A.; Meibohm, B.; Talcott, S. T.; Derendorf, H. *J. Agric. Food Chem*., **2008**, *56*, 7796 – 7802

37. Pacheco-Palencia, L. A.; Mertens-Talcott, S.; Talcott, S. T. *J. Agric. Food Chem.*, **2008**, *56:12*, 4631 – 4636

38. Cerd, B.; Toms-Barbern, F. A.; Espn, J. C. J. Agric. Food Chem., 2005, 53:2, 227 – 235

39. Von Weymarn, L. B.; Brown, K. M.; Murphy, S. E. *J. Pharmacol & Exper. Therap.*, **2005**, *316:1*, 295 – 264

40. Patten, C. J.; Smith, T. J.; Friesen, M. J.; Tynes, R. E.; Yang, C. S.; Murphy, S. E. *Carcinogenesis*, **1997**, *18:8*, 1623 – 1630

41. Bye, A.; King, H. K. *Biochem. Journal*, **1970**, *177*, 237 - 240